REVIEW

THE HIGH VOLTAGE ELECTRON MICROSCOPE
IN BIOLOGY

AUDREY M. GLAUERT

From the Strangeways Research Laboratory, Cambridge, England

The first published micrograph of a biological specimen photographed in a high voltage electron microscope (HVEM) appeared in a paper by Van Dorsten et al. in 1947, and it is consequently surprising that the HVEM does not play a greater role in biology 27 yr later. There are various reasons for this. The first prototypes were developed with the aim of enabling the investigator to examine thicker specimens than could be viewed at 100 kV. At the same time, however, the thin-sectioning technique was becoming established and consequently none of these early prototypes led to a commercial instrument (Glauert, 1972). Subsequently, the development of the HVEM was determined more by the needs of metallurgists and materials scientists rather than the needs of biologists, although the 1.5-MV microscope in Toulouse was constructed in the hope that it would make possible the examination of living cells (Dupouy et al., 1960). Results in this field have proved disappointing; even the best micrographs obtained so far reveal very little more internal detail of cells than can be seen with an ultraviolet microscope, and damage to living organisms during irradiation in the electron microscope is so fatal that any process that is observed is more correctly described as 'dying' than 'living'.

In spite of the apparently insuperable problems in obtaining electron micrographs of living cells, the HVEM still has great potentiality in biology, arising from its capability to produce *high resolution* images of *thick* specimens. This capability enables the examination of much thicker sections than can be viewed in conventional instruments operating up to 100 kV and, in combination with stereo viewing, has restored the third dimension in studies of a great range of biological material. Examining very thin sections over more than 25 yr has led microscopists to think of biological structures in terms of thin slices; the term 'mitochondrion' summons up the vision of the cross-sectional view rather than of a three-dimensional cylinder composed of interconnected membrane systems. This restoration of the third dimension in the appreciation of biological organization has been the major contribution of the HVEM so far.

The other promising line of investigation is the examination of hydrated (*not* living) specimens in the HVEM. Water is an essential constituent of all biological structures, and consequently it is of paramount importance to be able to examine specimens in the wet state, particularly when considering the molecular level of organization. Rapid progress has been made during the past few years in the development of suitable preparative and imaging techniques, and in the design of 'environmental cells', and there is no doubt that further advances in this field will soon be reported.

At present the few biologists who are using the HVEM are not all bringing the most fruitful problems to the microscope. For example, there is no point in obtaining a stereo view of a thick section unless an understanding of the three-dimensional structure of the embedded material will make a real contribution to the solution of a particular problem. The primary aim of this review is to indicate the capabilities of the HVEM and to

clarify the type of biological problem to which the HVEM can be expected to make a significant contribution. A short description of the microscope itself will be given, and will be followed by a more detailed discussion of the application of the HVEM to the study of thin specimens at high resolution and to the examination of thick specimens, ranging from thick sections to hydrated cells.

HIGH VOLTAGE ELECTRON MICROSCOPY

From the operator's point of view a high voltage electron microscope is merely a scaled-up version of a conventional 100 kV transmission electron microscope and has very similar controls. The optics of the microscope and the requirement for adequate shielding against X rays necessitate a relatively large and massive column, and consequently some of the adjustments have to be made by remote control. The high voltage generator and accelerator are contained in gas-filled pressure tanks mounted above the microscope, and the total

height required is such that the microscope has to be installed in a specially built or modified building.

The maximum operating voltage of most HVEMs is 1 or 1.2 MV, but microscopes operating up to 3 MV have been constructed in Toulouse and in Osaka, and a 10 MV microscope is under construction in Japan. Full instrumental details of HVEMs are given in reviews by Cosslett (1969, 1971, 1974 a, b), Dupouy (1968, 1973, 1974) and Hama (1973 a).

The main advantage of a high voltage electron microscope is that sharp images of *thicker* specimens can be obtained (Figs. 1 and 2), as a result of the greater penetrating power of high-energy electrons (Fig. 3) and the reduced chromatic aberration. In addition, higher resolution images of *thin* specimens can be obtained with reduced radiation damage. The main disadvantage is the reduction in contrast that accompanies increasing accelerating voltages (Fig. 4), but this is fairly easily overcome by the use of modified staining methods or by the application of dark-field imaging techniques (Fig. 4 d).
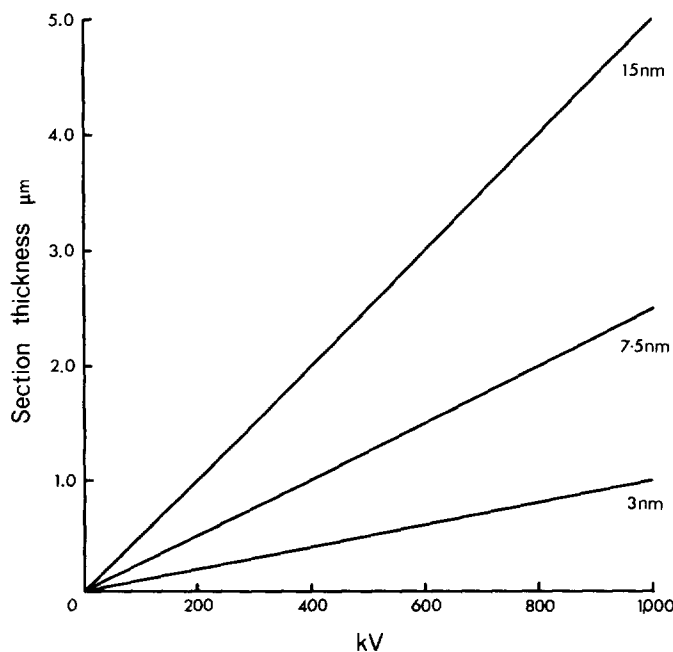

FIGURE 1   Graphs showing the relation between the *maximum* thickness of sections of rat muscle and accelerating voltage for three levels of resolution in the image (3 nm, 7.5 nm and 15 nm). For sections only 0.5 μm thick, 3-nm resolution is obtained at an accelerating voltage of 500 kV, while for sections 1.0 μm thick it is necessary to raise the voltage to 1000 kV for the same resolution. (Modified from Szirmae et al., 1971.)
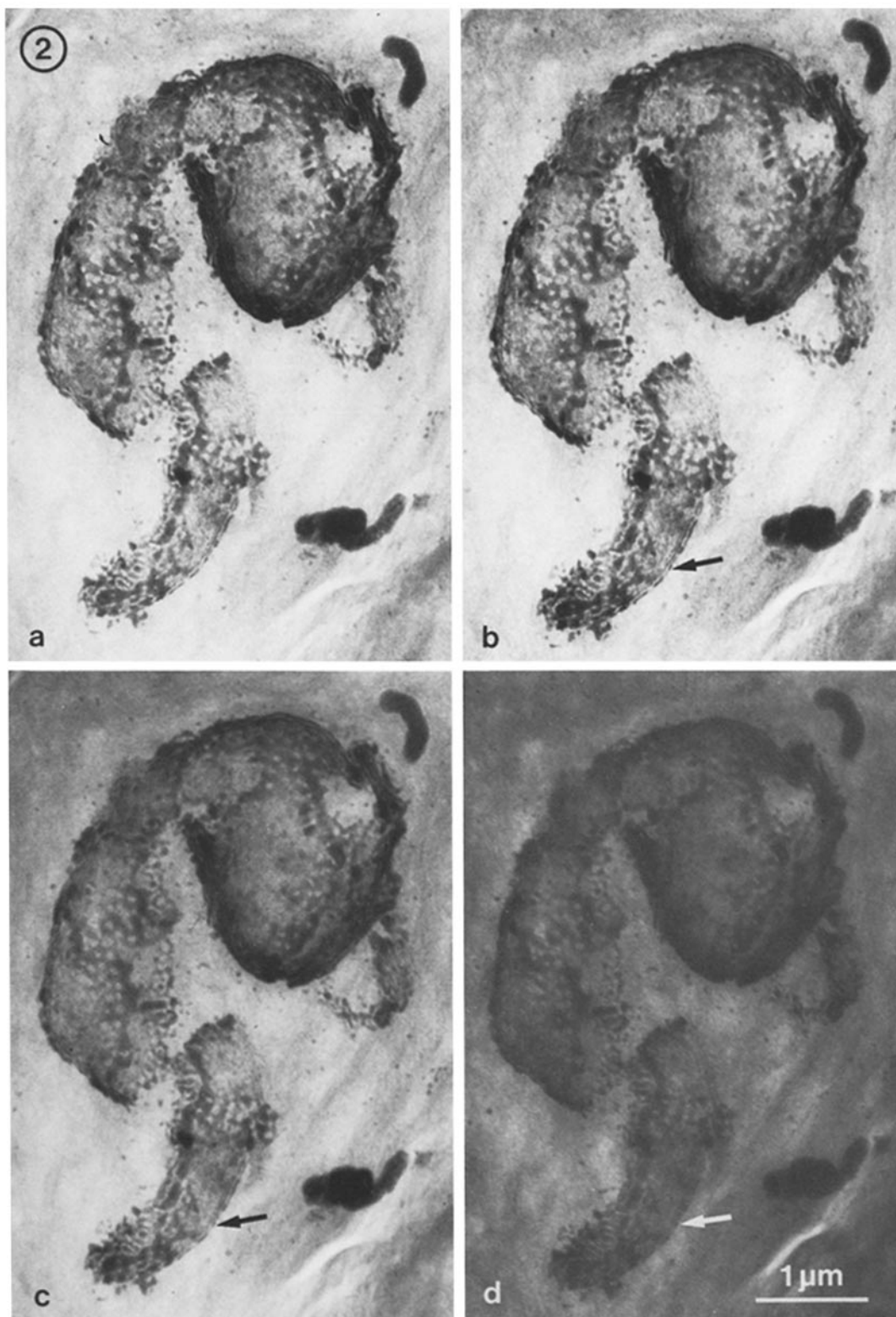
FIGURE 2   Section, 5 μm thick, of snail mucous gland stained by impregnation with osmium and photographed at different accelerating voltages. (a) 2 MV, (b) 1 MV, (c) 0.8 MV, (d) 0.5 MV. The image begins to lose definition at accelerating voltages below 1 MV (arrows), and is less sharp at 0.5 MV than at 0.8 MV. × 18,000. (From Favard et al., 1971, with copyright permission.)
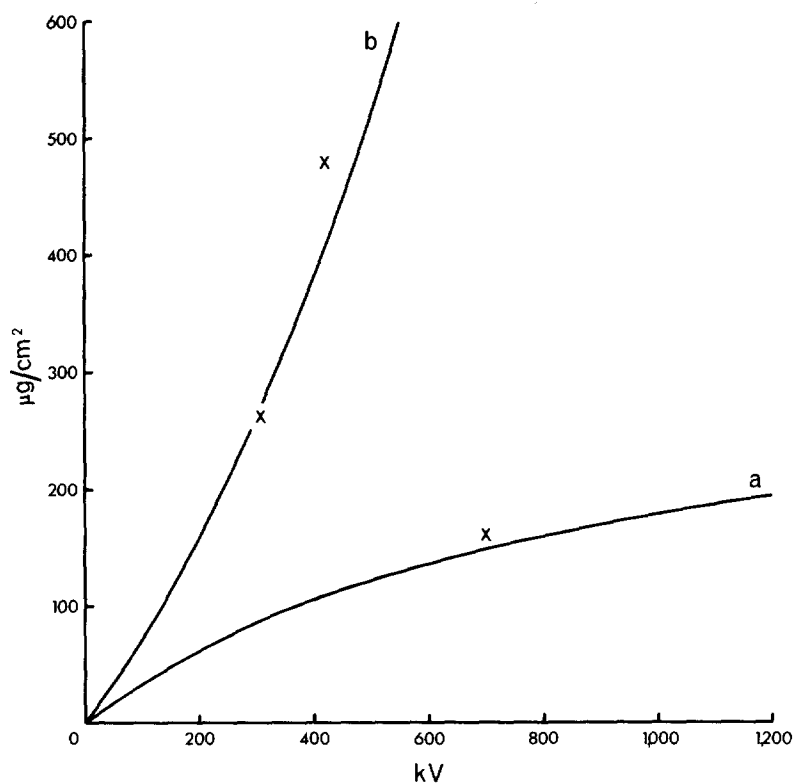
FIGURE 3   Graphs showing the relation between the thickness of a carbon film (measured in mass per unit area) allowing a certain transmission of electrons and kilovoltage, for two values, (a) and (b), of the angular aperture (γ) of the objective lens. (a) $\gamma = 1 \times 10^{-3}$; (b) $\gamma = 5 \times 10^{-3}$. (Modified from Cosslett, 1969.)

HIGH RESOLUTION MICROGRAPHS OF THIN SPECIMENS

Theoretically, it should be possible to obtain higher resolution with a HVEM than with a conventional transmission electron microscope as a consequence of the reduced spherical aberration, particularly in the dark-field mode of operation. For example, Cosslett (1969) estimates that the theoretical resolving power of a 1-MV microscope is about 0.1 nm, as compared with 0.2 nm for a 100-kV instrument. It seems probable, however, that the limit to resolution in the examination of biological specimens will be set not by the microscope itself, but by damage to the specimen during preparation and during irradiation in the microscope.

The problems arising from radiation damage have recently been reviewed by Glaeser (1974). He estimates that the limiting resolutions for polyethylene, l-valine, adenosine, and uranyl acetate-stained catalase are 5 nm, 11 nm, 4 nm and 1.3 nm,

respectively, at 100 kV. When recording the image no advantage is gained from low-beam intensity, because the damage is not dose dependent, and results are variable on reducing the specimen temperature. At high voltages the specimen 'lifetimes' are 2.5–3 times longer than at conventional voltages, and experimentally the damage in thin organic specimens appears to be less at 1 MV than at 100 kV for the same electron exposure. It is clear, however, that considerable modifications in conventional specimen preparation and imaging techniques will be required in order to utilize fully the potential resolution of high voltage electron microscopes (Glaeser, 1974; Parsons, 1974 a).

The relatively few papers so far published describing the results of studies of thin specimens at high resolution in the HVEM are listed in Table I. Hama and his colleagues (see references in Table I) are the only workers to have investigated the possibility of obtaining high resolution images of thin sections. They have reported that the quality of the images was higher than that obtained at
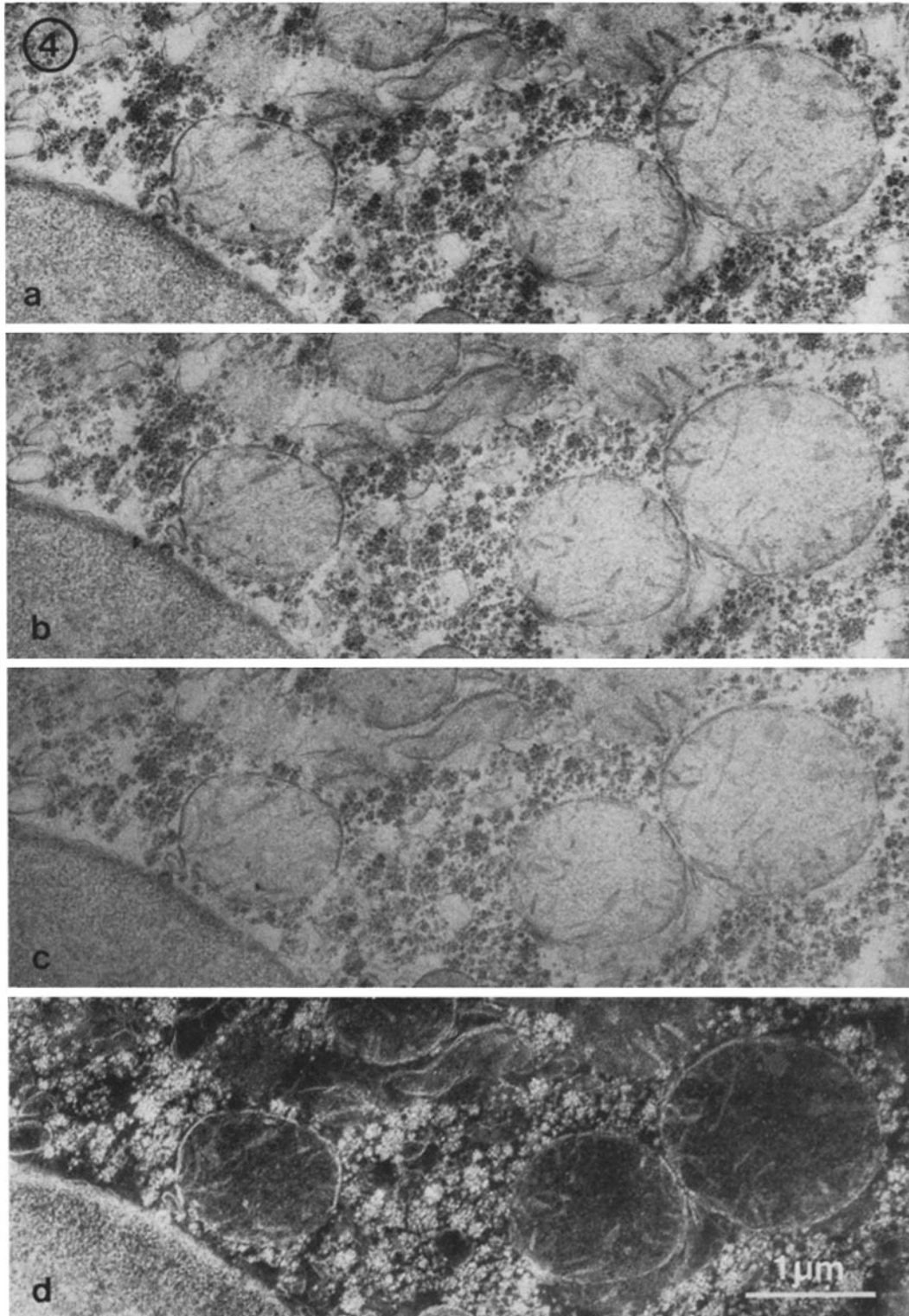
FIGURE 4 Thin (80 nm) section of rat liver photographed at different accelerating voltages. (a) 0.5 MV, (b) 1 MV, (c) 2 MV, and (d) in dark-field. The contrast decreases as the accelerating voltage increases. × 20,000. (From Favard et al., 1971, with copyright permission.)

Specimen	Thickness	Accelerating voltage	Reference
Sections			
Chicken gizzard; smooth muscle	60 nm	500 kV ⎫	
Mouse mast cells	50 nm	500 kV ⎬	Hama and Porter (1969)
Rat skeletal muscle	60 nm	500 kV ⎟	
Goldfish saccular macular	60 nm	500 kV ⎭	
Mouse stomach; parietal cells	60 nm	800 kV	Hama and Nagata (1970 *a*)
Smooth muscle membranes	80 nm	800 kV	Nagata and Hama (1969)
Insect flight muscle	60 nm	800 kV	Hama (1973 *a*)
Frog skeletal muscle (unstained, dark field)	75–100 nm	2.8 MV	Massover, in Dupouy (1973); Massover (1974)
Isolated particles			
Bacterial flagella, dark-field		1 MV	Dupouy et al. (1969)
Ferritin, unstained, bright- and dark-field		1 MV and 3 MV	Massover (1972 *a*); Massover et al. (1973)
Bacterial cell walls, dark-field		3 MV	Dupouy (1973)

Note: this table gives details of published micrographs.

conventional voltages; subunits were detectable in cross sections of the thick filaments of striated muscle (Hama and Porter, 1969), and unit membranes were more clearly resolved, as confirmed by densitometer tracings (Hama and Nagata, 1970 *a*).

Massover, working with the 3 MV Toulouse microscope, has overcome the problems arising from the low signal-to-noise ratio in images of thin specimens examined at high voltages by using the dark-field (central beam stop) methods developed by Dupouy (1968; 1973). Excellent definition was obtained of the myofilaments in thin sections of skeletal muscle (Massover, 1974) (Fig. 5), and a granular substructure was apparent in some glycogen particles. Massover (1972 *a*) and Massover et al. (1973) have also examined unstained ferritin molecules deposited on ultrathin carbon films in both bright- and dark-field images. The iron-rich cores of the ferritin molecules were visible in bright field at 1–3 MV, but with very low contrast. In dark field at 1 MV, halos were observed around some ferritin cores, possibly representing unstained apoferritin. At 3 MV most of the cores appeared unstructured, but others appeared to contain one or more granules of varying size, shape and intensity (Figs. 6 and 7). A regular geometric arrangement of these granules was very rare.

Dupouy's (1968; 1973) dark-field imaging technique has also been used to obtain remarkable pictures of bacterial flagella (Dupouy et al., 1969) and of bacterial cell walls (Dupouy, 1973). The cell

walls were lightly stained with phosphotungstic acid, and a regular periodic structure was visible (Fig. 8).

These first results are sufficiently promising to indicate that the HVEM will eventually make a significant contribution to studies at very high resolution. It is of interest that many of the high resolution projects at present under development in various countries include the use of high accelerating voltages in the range of 250–600 kV (see review by Cosslett, 1974 *a*).

EXAMINATION OF THICK SECTIONS

The information obtained on the three-dimensional organization of biological specimens from examining stereo images of thick sections is the major contribution so far made by the HVEM to biology. The main reason for the popularity of this approach is the fact that the techniques for the preparation of thick sections involve only simple modifications of the widely used thin-sectioning technique. These modifications include the development of special staining methods to provide sufficient contrast at high accelerating voltages, and the application of stereo viewing techniques to obtain the final three-dimensional image.

The Preparation of Thick Sections for the HVEM

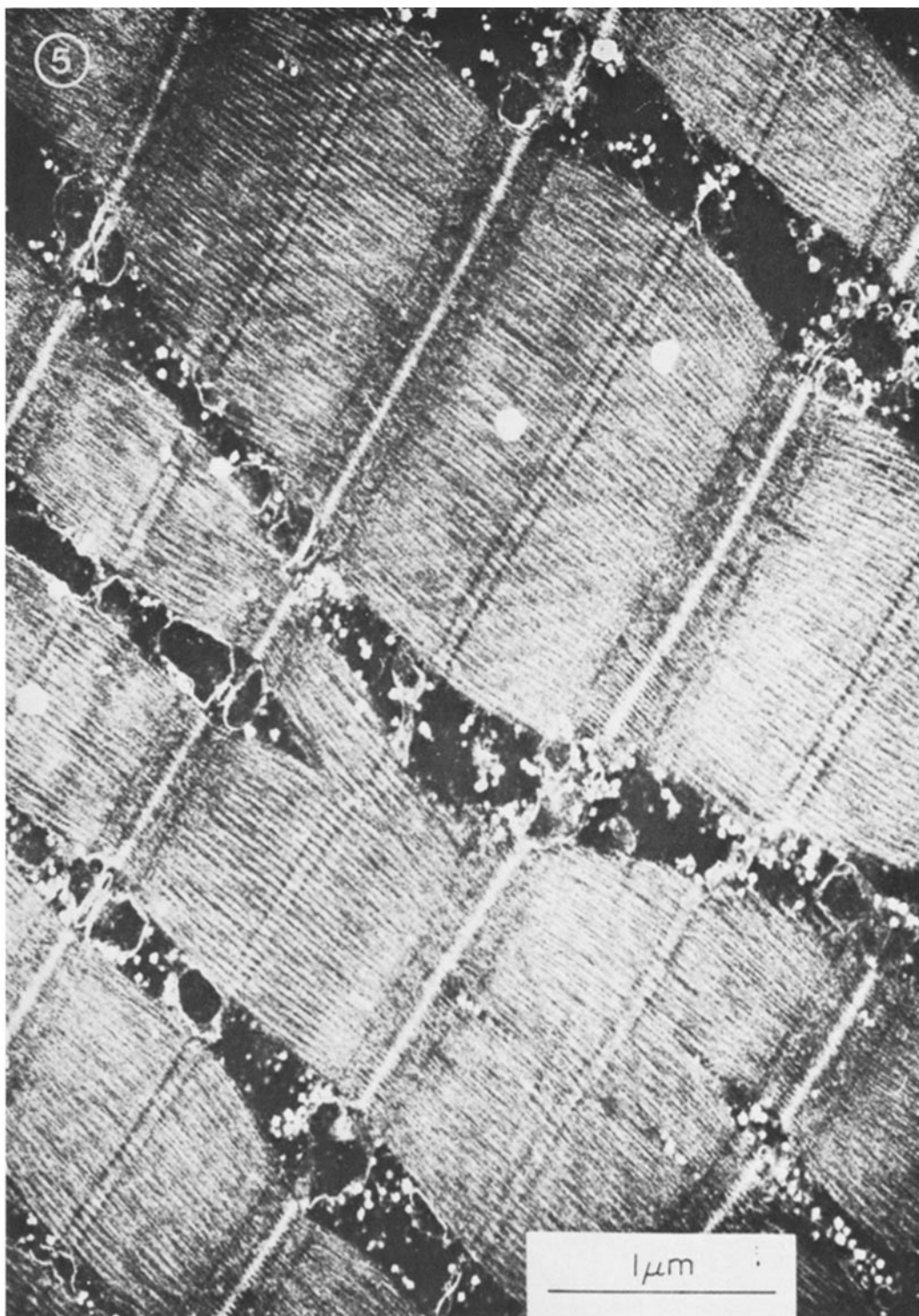The fixation, embedding, and staining methods that have proved successful for thick sections are

FIGURE 5   Dark-field image of a thin (75–100 nm) section of rat skeletal muscle. 2.8 MV. × 35,000. (From Dupouy, 1973, with copyright permission.)
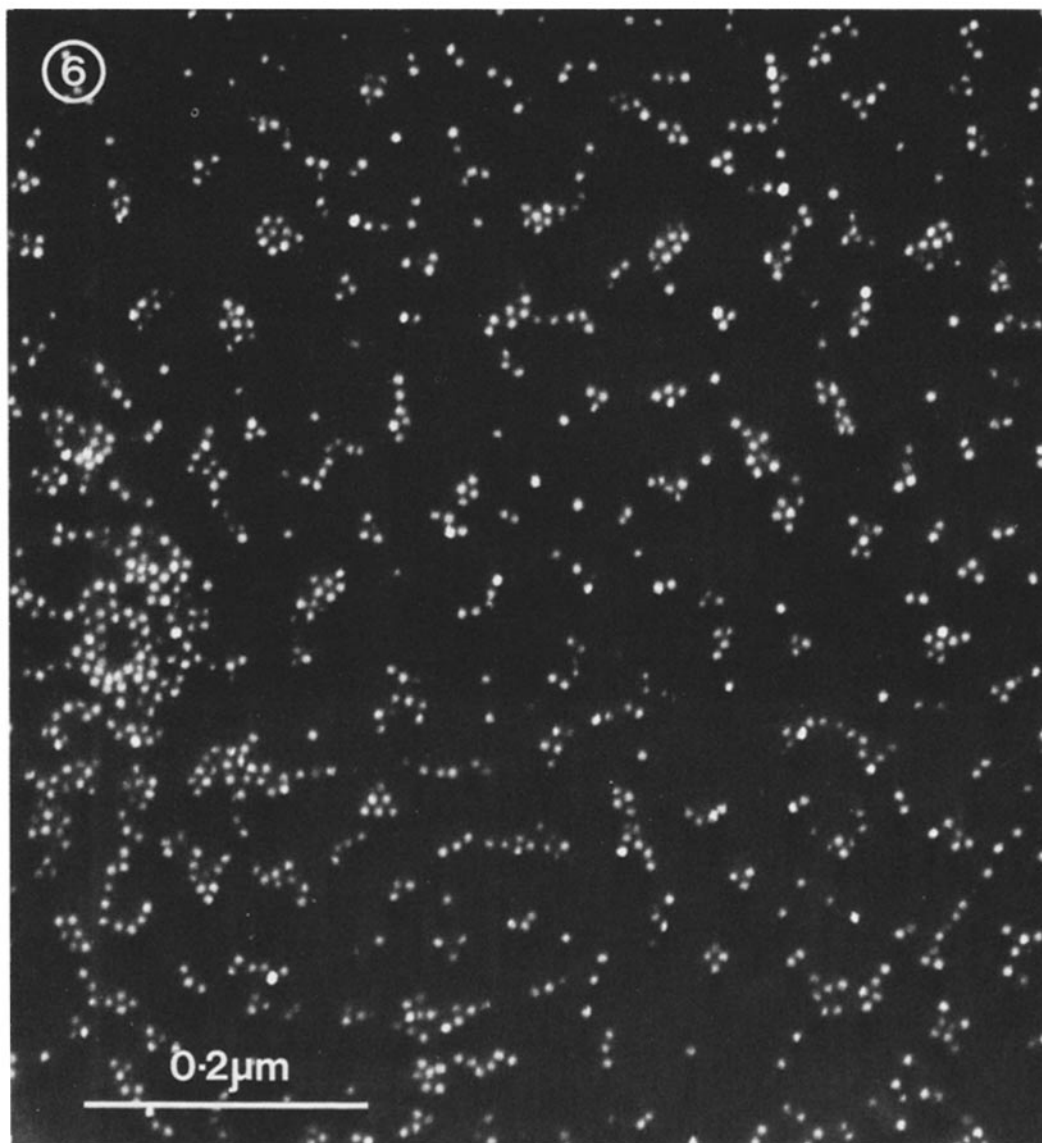
FIGURE 6 Dark-field image of unstained ferritin molecules on a thin carbon film. 3 MV. × 191,000. (From Massover et al., 1973, with copyright permission.)

listed in Table II. Standard fixation and embedding methods are used, and block staining before or during dehydration is recommended to provide contrast throughout the depth of the section. The alcoholic uranyl acetate stains provide greater contrast than the aqueous ones (Locke et al., 1971), but may make the specimens more difficult to section.

Thick sections are prepared on conventional ultramicrotomes using a diamond knife if possible.

With glass knives the surface of the section may be damaged during cutting, although Favard and Carasso (1973) have shown that this damage can be avoided by cutting a few thin sections between thick ones. Thick sections which have been compressed during cutting do not usually respond to treatment with chloroform or xylene vapours, but some sections will expand by themselves if left floating in the trough for a short time (Massover 1972 b). Rambourg (1973, personal communica-
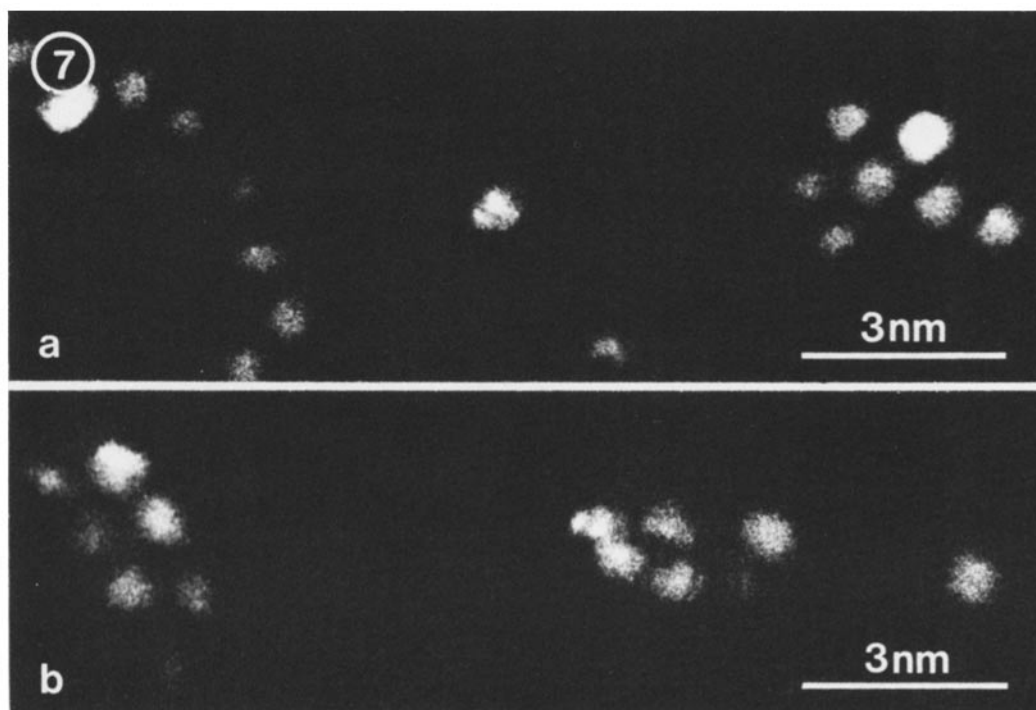
FIGURE 7   (a) and (b). Enlargements of regions of Fig. 6 showing structure in some ferritin cores. 3 MV. ×
902,000. (From Massover et al., 1973, with copyright permission.)

tion) suggests cutting thick (1–7 μm) sections from blocks which are only partially polymerized (15-h incubation for Epon 812). Polymerization is then completed by incubation for a further 12 h before cutting thin sections.

Sections up to 1 μm thick can be mounted on standard 200- or 300-mesh grids. Thicker sections tend to become detached from the grid during staining or during viewing in the microscope, and are best mounted in folding oyster grids (Favard et al., 1971), care being taken to press the two halves of the grid firmly together. Adhesion of sections to grids can be enhanced by dipping the grids in a solution of 1% isobutylene in xylol to deposit a sticky layer on the grid bars (Drummond, 1950).

Section Staining

Thick sections are stained by immersing them in the staining solutions to enable the stain to penetrate from both sides. Again, alcoholic solutions of uranyl acetate are to be preferred to aqueous ones, and penetration can be improved still further by staining at a high temperature (e.g. 60°C) (Locke and Krishnan, 1971; Carasso et al., 1973). For lead staining, the standard lead citrate solution of

Venable and Coggeshall (1965) penetrates well, and it is only necessary to increase the staining time as the section thickness increases. Carasso et al. (1973) have shown that the rate of penetration is about 2.5 μm/h for Araldite sections, and that it can be made even faster, and the staining more homogeneous, by the addition of a detergent (0.3% Tween 80) to the staining solution. Surface deposits may form during prolonged staining but are easily removed by treatment with 0.05% nitric acid for about 1 min (Favard and Carasso, 1973). Hama and Kamino (1974) recommend coating the sections with a layer of carbon after staining.

Selective Staining

The routine method of staining with uranyl acetate, followed by lead citrate or phosphotungstic acid, is designed to provide staining of biological material so that its overall architecture can be studied (Fig. 9). For certain special purposes, however, there is considerable advantage in staining only the organelle or region of interest. With such selective stains, much thicker sections can be examined with profit since the stained elements are seen against an empty unstained background.
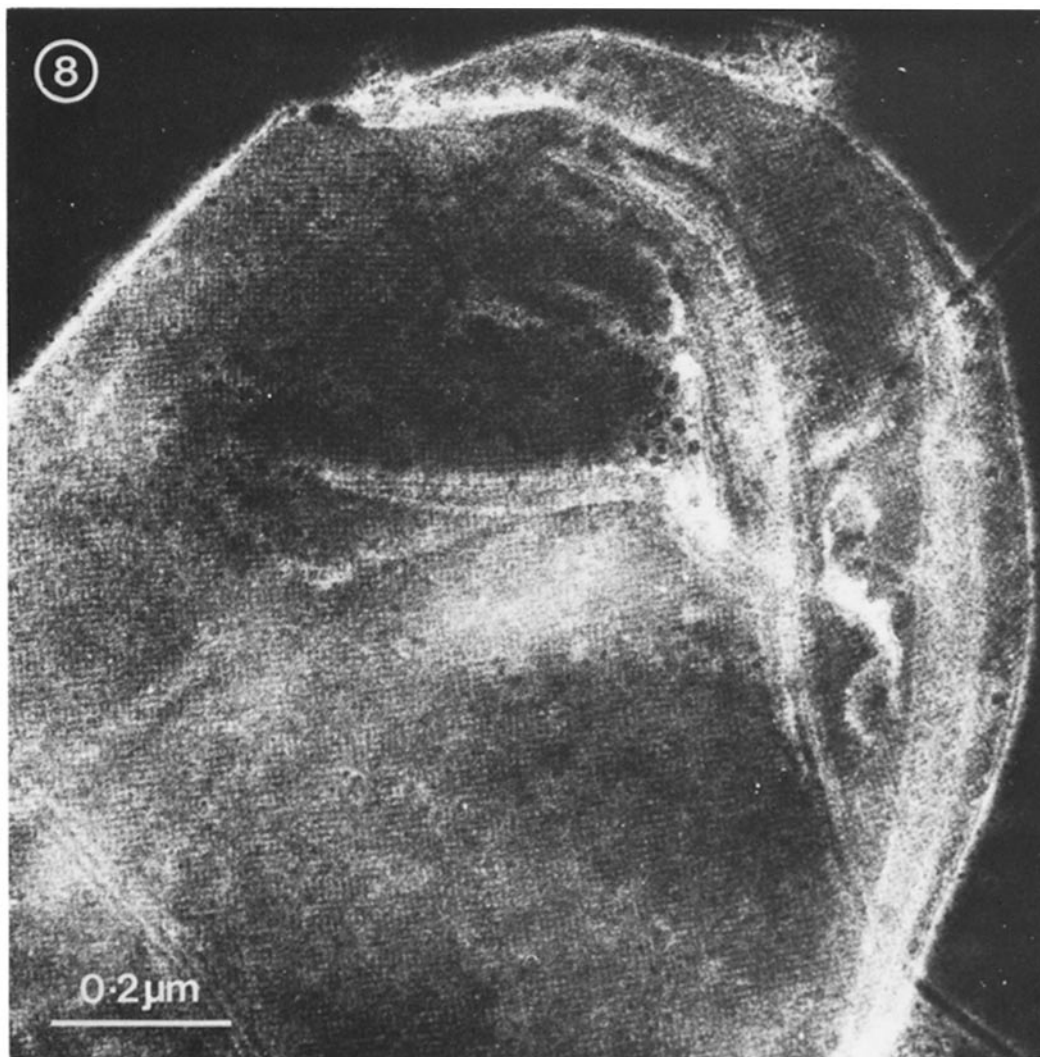
FIGURE 8 Dark-field image of the cell wall of *Pseudomonas putida* showing a regular periodic structure. 3 MV. × 120,000. (From Dupouy, 1973, with copyright permission.)

The most widely used selective staining method is the osmium impregnation technique of Friend and Murray (1965). This method has been used extensively by Rambourg and his colleagues in studies of the forming face of the Golgi apparatus, and they have shown that reasonably sharp images of 0.5–1.0-μm thick sections can be obtained in a conventional electron microscope operating at 100 kV (Rambourg and Chrétien, 1970; Rambourg et al., 1973), while sections as thick as 7 μm can be studied at 1 MV (Rambourg et al., 1973; 1974) (Fig. 10). In similar studies of the osmium impregnation of the Golgi apparatus, Carasso, Favard,

and their co-workers (Carasso et al., 1971; Favard et al., 1971; Favard and Carasso, 1973; Carasso et al., 1974) examined tissues after osmium staining alone (Figs. 11 and 12), or after osmium staining followed by block staining with uranyl acetate. After this double staining, the membranes of the maturing face of the Golgi apparatus are also visible and their relationship to the osmium-stained membranes of the forming face can be studied.

The three-dimensional distribution of enzymes can be examined in thick sections of tissues stained with specific cytochemical stains in the absence of

any counterstaining. For example, Carasso and Favard used Gomori's lead stains for acid-phosphatase (Carasso et al., 1971; Favard et al., 1971), and for glucose-6-phosphatase (Favard and Carasso, 1973) (Fig. 13) to locate these enzymes in the Golgi apparatus and the endoplasmic reticulum, respectively.

Other selective stains that have been tested include silver impregnation for the Golgi apparatus (Palay and Chan-Palay, 1973) and for neurofibrils (Favard and Carasso, 1973) (Fig. 14), and bismuth subnitrate for cell surfaces (Peachey et al., 1974). In addition, tracers such as thorium dioxide (Favard et al., 1971) and ruthenium red and peroxidase (Yamada and Ishikawa, 1972) have been used to stain cellular compartments which are in continuity with the extracellular space.

Examination of Thick Sections in the HVEM

When commencing a study of thick sections by HVEM, it is advisable to start by examining relatively thin sections (e.g. 0.5 μm) and to increase the thickness only after becoming familiar with the specimen. The overlap of detail in depth in a thick section if often confusing, and in very thick sections some structures may no longer be recognisable (Favard et al., 1971) (Fig. 15). Similarly, it is not profitable to immediately use the highest accelerating voltage available, since this may lead to an unnecessary loss of contrast (Fig. 4) without any accompanying gain in the clarity of the image (Fig. 1). Except for very dense specimens an accelerating voltage of 500 kV is adequate for 0.5-μm sections, and gives all the benefits of higher contrast in the image.

The stability of thick sections in the HVEM has not yet been studied in detail. Sections are often observed to move under the electron beam (e.g. Massover, 1972 b), as a result of poor adhesion between the sections and the supporting grid or as a result of local heating of the section. Favard and Carasso (1973) have shown that this temperature rise is accompanied by a loss of transparency of the sections when viewed in the light microscope and by a decrease in section thickness. These effects increase with section thickness up to about 10 μm and are probably related to the rate at which heat is conducted away from the area under investigation. Above 10 μm, the loss in thickness is irregular and craters form under the beam. Hama (1973 a) has concluded that the limitation to the thickness

of sections for the HVEM is set by temperature rises and radiation damage rather than by inadequate transmission or resolution resulting from chromatic aberration.

Stereo Viewing of Thick Sections

The method of obtaining a stereo pair of images of a thick section is simple. An area is selected and a micrograph taken, and then the specimen is tilted through the required angle and a second exposure made. Unless the selected region is on the axis of tilt, the image will move during tilting and go out of focus, the extent depending on the distance of the region from the tilt axis. Consequently, it is necessary to examine the position of the image on the screen very carefully so as to be able to bring it back to exactly the same position for the second exposure. The tilt angle is chosen so that the parallax between the final images to be viewed is less than 5 mm at a distance of 25 cm, and depends on the thickness of the section, the magnification of the final image, and the magnification and working distance of the stereo viewer. Curves giving the optimum tilt angles for stereo viewing have been published by Hudson and Makin (1970) (Fig. 16), and the criteria for selecting images for stereo recording are discussed by Beeston (1973) and Thomas et al. (1974). The basic requirement is that the two pictures should match in detail, except for the parallax. Thomas et al. (1974) also outline methods for making stereoscopic measurements and for preparing stereo slides for projection. Techniques enabling the preparation of stereo models are available and have been used by Rambourg et al. (1973) (Fig. 17).

Achievements of the Thick-Sectioning Technique

The major achievement of the HVEM in the study of thick sections has been the mapping of the forming face of the Golgi apparatus using the osmium impregnation technique. Rambourg and his colleagues (Rambourg et al., 1973, 1974) have clearly demonstrated that the apparently isolated saccules located at the forming face of stacks of Golgi lamellae are in fact part of a continuous convoluted structure made up of a tubular polygonal network (Figs. 10 and 17). Carasso, Favard, and their co-workers have recently extended their study of osmium impregnation of animal cells (Fig. 12) to include botanical material and have

TABLE II
Studies on Thick Sections

Specimen	Fixation	Impregnation or block staining	Embedding medium	Section thickness (μm)	Section staining	Stereo tilt	Accelerating voltage	Reference
Grasshopper spermatocytes	OsO₄	-	M	1.0	U-Mg-Ac; Pb	-	1 MV	Ris (1969)
Dinoflagellate chromosomes	P + G; OsO₄	UA	E + A	1.0	U-Mg-Ac; Pb	8–10°	1 MV	Ris (1969)
Rodent retina	?	?	M	0.5	UA; Pb	16°	750 kV	Nagata et al. (1969)
Mouse capillaries	OsO₄	-	E	0.5	UA; Pb	16°	500 kV	Hama and Porter (1969)
Mouse mast cells	or	-	E	0.5	UA; Pb	16°	500 kV	Hama and Porter (1969)
Bat retinal rods	G; OsO₄	-	E	0.5	UA; Pb	16°	500 kV	Hama and Porter (1969)
Mouse tracheal epithelium	OsO₄; G; OsO₄	UA	E	1.0	UA(alc); Pb	16°	800 kV	Hama and Nagata (1970 b, c); Hama (1973 a)
Drosophila salivary gland	G; OsO₄	UA	E	1.0	UA(alc); Pb	16–20°	800 kV	Hama (1973 a)
Lateral line organ of sea eel	G + OsO₄	UA	E	1.0	UA(alc); Pb	16°	800 kV	Hama (1973 b); Hama and Kamino (1974)
Snail mucous gland	OsO₄	OsO₄	A	0.4–5.0	-	10°	0.5–2 MV	Carasso et al. (1971); Favard et al. (1971); Carasso et al. (1973); Favard and Carasso (1973); Carasso et al. (1974).
Mouse epididymis	OsO₄	OsO₄	A	2.0	-		1 or 2 MV	
Mouse epididymis	OsO₄	UA(alc)	A	2.0	-		1 or 2 MV	
Rat epididymis	OsO₄	OsO₄	A	1.5; 2.0	-	10°	2.5 MV	
Rat liver	OsO₄	UA; Pb	A	1; 2; 10	-		1–2 MV	
Rat liver	OsO₄	-	A	2.0	UA		2.5 MV	
Rat liver	OsO₄	-	A	2.4	Pb		2.5 MV	
Rat liver	?; Gomori (G-6-Ph)	-	A	1; 2	Pb	20°	2.5 MV	
Rat digastric muscle	?; Gomori (G-6-Ph)	-	A	1.0	-		2.0 MV	
Triton ovaries	OsO₄	PTA (alc)	A	3.0	-		1 MV	
Frog testis	G; Gomori (AcPh); OsO₄	-	A	2.0	-		2.5 MV	
Hen serous gland	?	-	A	5.0	PTA(alc)		2.5 MV	
Quail tubular gland	G; OsO₄	-	A	1.2; 2.9	Pb		2.5 MV	
Quail tubular gland	G; OsO₄	-	A	2.0	UA(alc)	20°	2.5 MV	
Leech nerve	?	Ag	A	2.0	-	20°	2.5 MV	
Leech nerve	?	Zn-1-Os	A	1.4; 1.8	-		2.5 MV	Carasso et al. (1971); Favard et al. (1971); Carasso et al. (1973); Favard and Carasso (1973); Carasso et al. (1974).
Ciliates (thorotrast)*	G; OsO₄	-	A	2.0	-		1 MV	
Ciliates	G; Gomori (Ca++); OsO₄	-	A	2.0	-		1 MV	
Tetrahymena	G; OsO₄	-	A	1; 3	UA(alc)	10°	2.5 MV	
Tetrahymena	G; OsO₄	-	A	1.2	Pb	10°	2.5 MV	
Plant cells	OsO₄	OsO₄	A	0.5; 1; 2	-		2.5 MV	
Plant cells	G; Gomori (AMPh)	-	A	2; 4	-		2.5 MV	

Specimen	Fixation	PTA(alc)	Embedding	Section (μm)	Stain	Tilt	Voltage	Reference
Frog sartorius muscle	G; OsO₄		A	0.5	–	–	1 MV	Mayo and Beeston (1971)
Red cell membranes	G; OsO₄	UA	A	3.0	UA; Pb	8°	1 MV	Glauert (1971)
Chick limb bones	G; OsO₄	UA	A	0.5; 1.0	UA; Pb	12–16°	1 MV	Glauert (1972); Glauert and Mayo (1973)
Silkworm spermatocytes	G; OsO₄		?	0.3; 1.0	UA; Pb	10–20°	1 MV	King and Akai (1971)
Rat psaos muscle	G; OsO₄		E + A	0.5–5.0	UA(alc); Pb	–	up to 1 MV	Szirmae et al. (1971)
Mouse kidney (RR)*	?		E	3.0	–	16–20°	1 MV	Yamada and Ishikawa (1972)
Mouse cardiac muscle (Per)*	?		E	1.0	–	16–20°	1 MV	Yamada and Ishikawa (1972)
Frog liver	?	UA	E	1.0	?	–	1 MV	Massover (1972 b)
Frog oocytes	G; OsO₄	UA	E	1.0; 2.0	UA; Pb	–	1 MV	Massover (1973)
Rat nerve	OsO₄		E	3.0; 7.0	–	14°	1 MV	Rambourg et al. (1973)
Spinal ganglion	OsO₄		E	1.0; 5.0	–	14°	1 MV	Rambourg et al. (1974)
Mouse epididymis	OsO₄		E	5.0	–	14°	1 MV	Rambourg et al. (1974)
Mouse testis	OsO₄		E	6.0	–	14°	1 MV	Rambourg et al. (1974)
Celery petioles; (collenchyma cell walls)	G; OsO₄		E	0.5; 1.0	UA; Pb	5–10°	1 MV	Cox and Juniper (1973 a, b)
Monkey and rat cerebellar cortex	G + P, or F	OsO₄	A	1; 3; 5	–	–	1 MV	Palay and Chan-Palay (1973)
Fish chromatophores	?	?	?	0.25	–	–	1 MV	⎫
Frog skeletal muscle	G + TA; OsO₄		?	0.5	BSN	–	1 MV	⎬ Peachey et al. (1974)
Tetrahymena	?	?	?	0.25; 0.5	–	–	1 MV	⎪
Green algal nucleus	?	?	?	0.5	–	–	1 MV	⎭

RR, ruthenium red; per, peroxidase; *, stain used as a tracer; P, paraformaldehyde; G, glutaraldehyde; G-6-Ph, glucose-6-phosphatase; AcPh, acid phosphatase; AMPh, adenosine mono-phosphatase; F, formaldehyde; TA, tannic acid; UA, uranyl acetate; (alc), alcoholic; PTA, phosphotungstic acid; M, methacrylate; E, Epon; A, Araldite; U-Mg-Ac, uranyl magnesium acetate; BSN, bismuth subnitrate; ?, method not described.
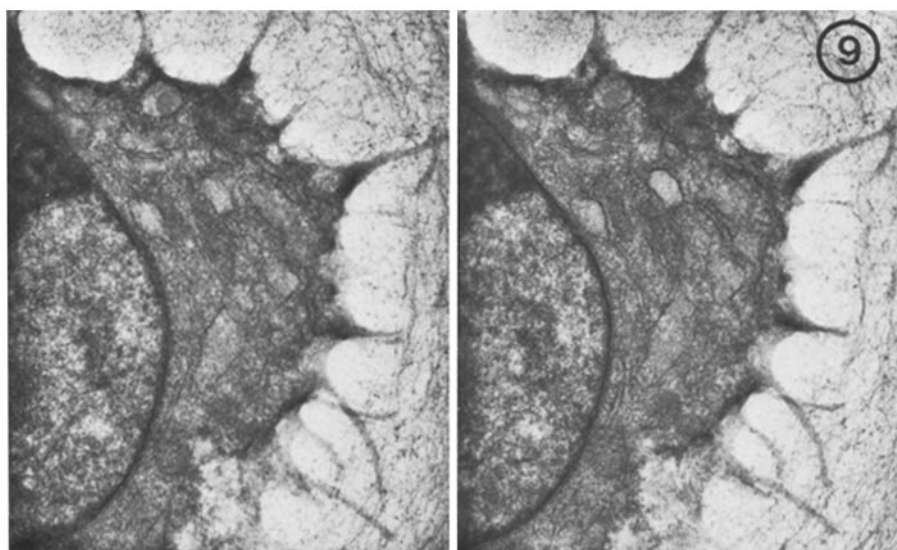Note: the table gives details of published micrographs.

FIGURE 9   Stereo pair of micrographs of a 0.5-μm thick section of a chondrocyte in an embryonic chick limb-bone; block stained with uranyl acetate, section stained with alcoholic PTA. General staining of cell structures is observed. 1 MV. Stereo tilt angle 16°. × 10,000. (Unpublished micrograph from a study by Audrey M. Glauert, H. Clarke Anderson, and C. R. Mayo.)
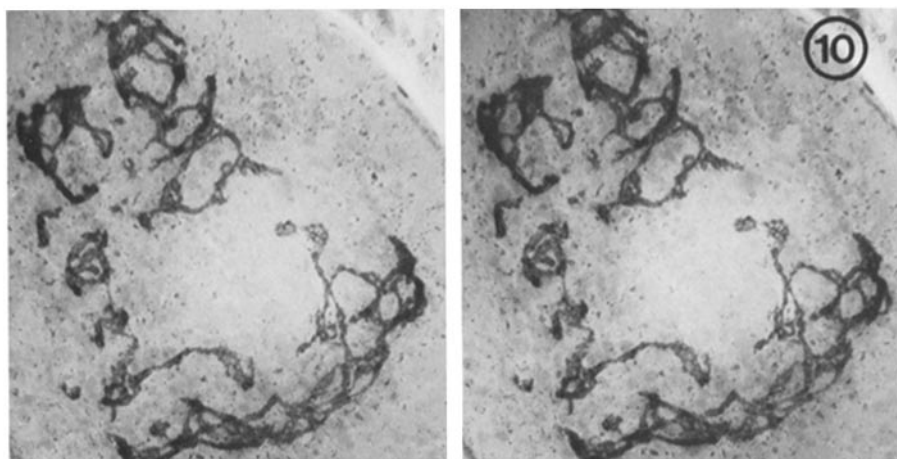

FIGURE 10   Stereo pair of micrographs of a 5-μm thick section of the Golgi apparatus in a small nerve cell of a mouse spinal ganglion; impregnated with osmium. 1 MV. Stereo tilt angle 14°. × 4,500. (From Rambourg et al., 1974, with copyright permission.)

shown that the endoplasmic reticulum (ER) is stained as well as the Golgi apparatus (Carasso et al., 1974). In meristematic cells of castor oil plant roots in interphase the nuclear envelope and its pores can be observed, in addition to the numerous points of origin of the ER (Fig. 11). Favard and Carasso have also demonstrated the ability of the HVEM to reveal the three-dimensional distribution of enzymes (Fig. 13), and of intracellular compartments that are in continuity with the extracellular space (Favard et al., 1971) (see also Yamada and Ishikawa, 1972).
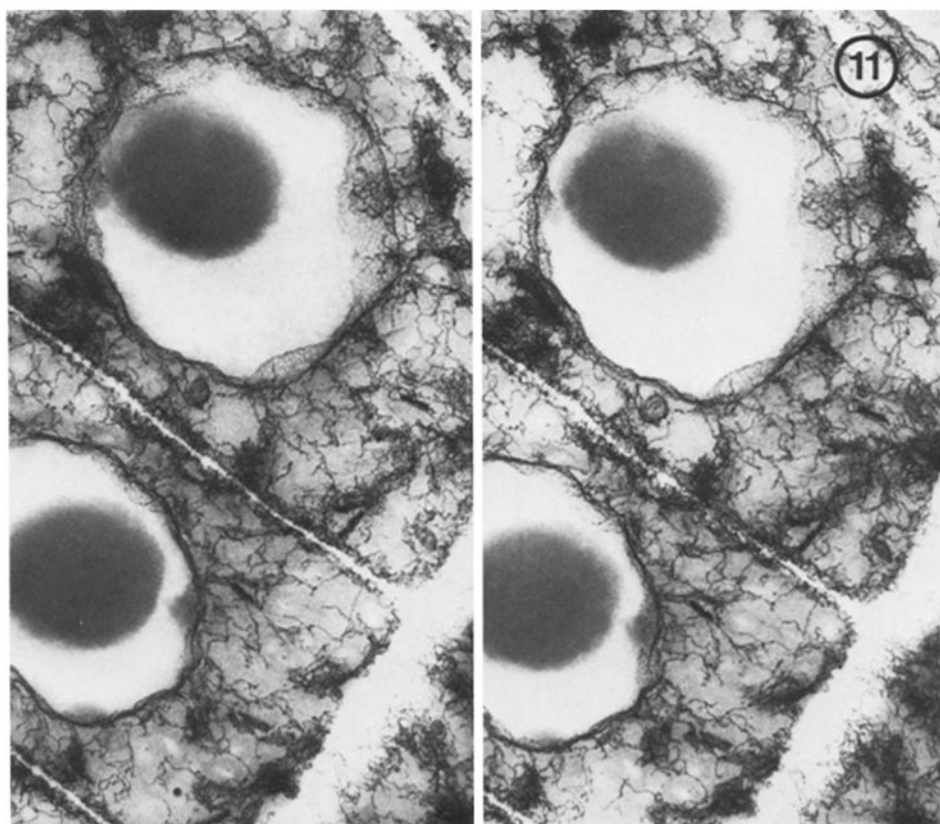
FIGURE 11   Stereo view of a 1-μm thick section of meristematic cells of a castor oil plant root in inter-
phase. Osmium impregnation reveals both the Golgi apparatus and the endoplasmic reticulum. The nuclear
envelope and its pores can be seen, as well as the numerous points of origin of the endoplasmic
reticulum. 2.5 MV. Stereo tilt angle 10°. × 7,500. (Unpublished micrographs from a study by N. Carasso,
N. Poux, and P. Favard.)

In many of the other published studies of thick
sections the three-dimensional image has proved of
value in the elucidation of the interrelationships of
membrane systems in such diverse specimens as
celery petioles (Cox and Juniper, 1973), chick limb
bone cells (Glauert and Mayo, 1973), bat retina
(Hama and Porter, 1969), the lateral line organ of
the sea eel (Hama and Kamino, 1974), and frog
oocytes (Massover, 1973), to quote just a few
studies from those listed in Table II. In addition,
as pointed out by Cox and Juniper (1973 a), stereo
viewing of thick sections can give face or oblique
views of membranes (Fig. 18), which are effectively
impossible to obtain by ultrathin sectioning. Such
views provide the opportunity of comparing, for
the first time, the membrane structure seen in
fixed, embedded, and positively stained tissue with

that seen in negatively stained or freeze-etched
preparations.

Two other applications of the thick-sectioning
technique have been suggested. Firstly, the exami-
nation of a few *serial* thick sections enables
three-dimensional models of quite large structures
to be constructed very easily (Hama, 1973 b;
Hama and Kamino, 1974). Secondly, the HVEM
can be used to examine autoradiographs of thick
sections (King and Akai, 1971; Peachey et al.,
1974), with the advantages of less intense labeling
and shorter exposure times than are required with
thin sections.

INTACT CELLS AND ORGANELLES

Some cells and organelles are thin enough to be
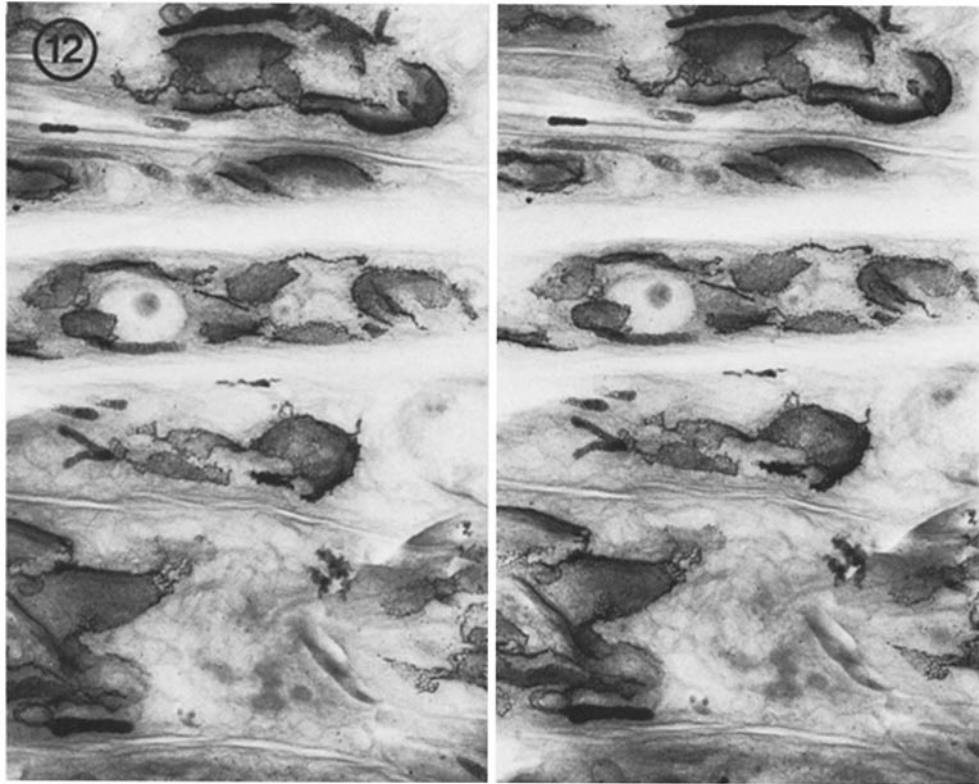viewed directly in the HVEM without the need for

FIGURE 12 Stereo view of a 1.5-μm thick section of osmium-impregnated snail mucous gland showing the reticular structure of the forming face and tubules of the Golgi apparatus. 2.5 MV. Stereo tilt angle 10°. × 6,500. (From Favard and Carasso, 1973, with copyright permission.)
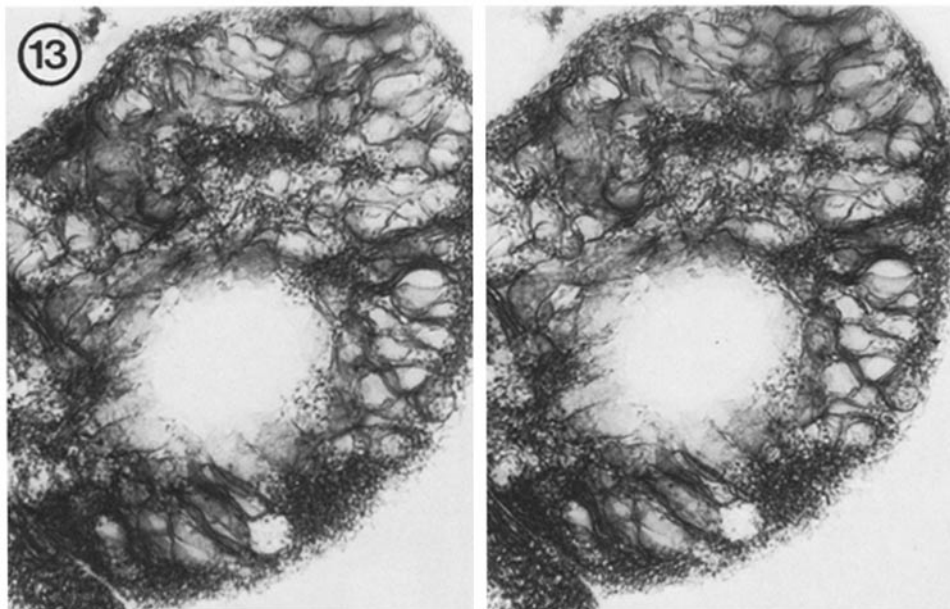

FIGURE 13 Stereo view of a 2-μm thick section of a rat liver cell stained for glucose-6-phosphatase by Gomori's method. The cisternae of the endoplasmic reticulum contain the reaction product. 2.5 MV. Stereo tilt angle 20°. × 6,500. (From Favard and Carasso, 1973, with copyright permission.)
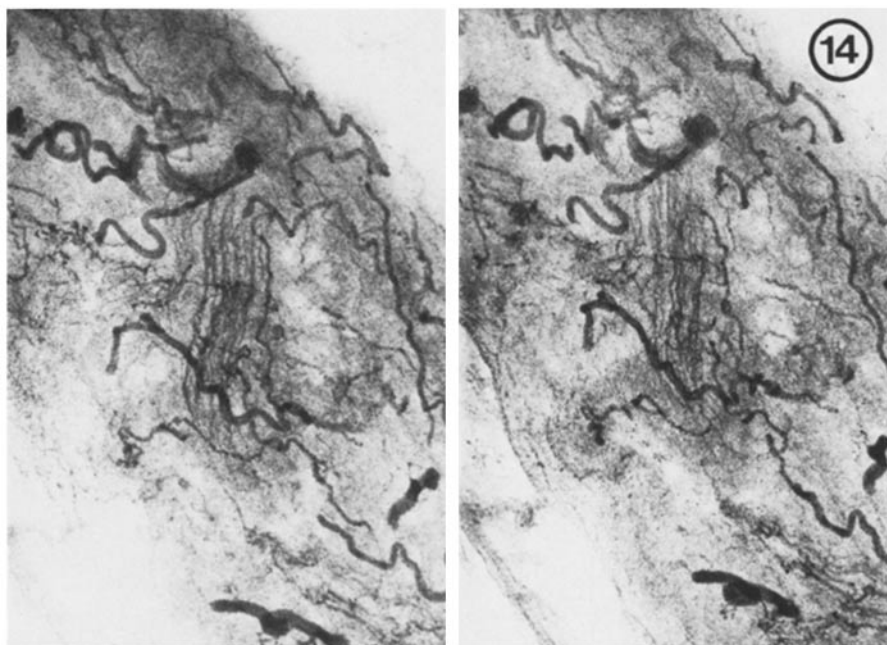
FIGURE 14 Stereo view of a 2-μm thick section showing neurofibrils in a cell of the leech ventral nerve-chain. Silver impregnation by Cajal's method. 2.5 MV. Stereo tilt angle 20°. × 6,500. (From Favard and Carasso, 1973, with copyright permission.)
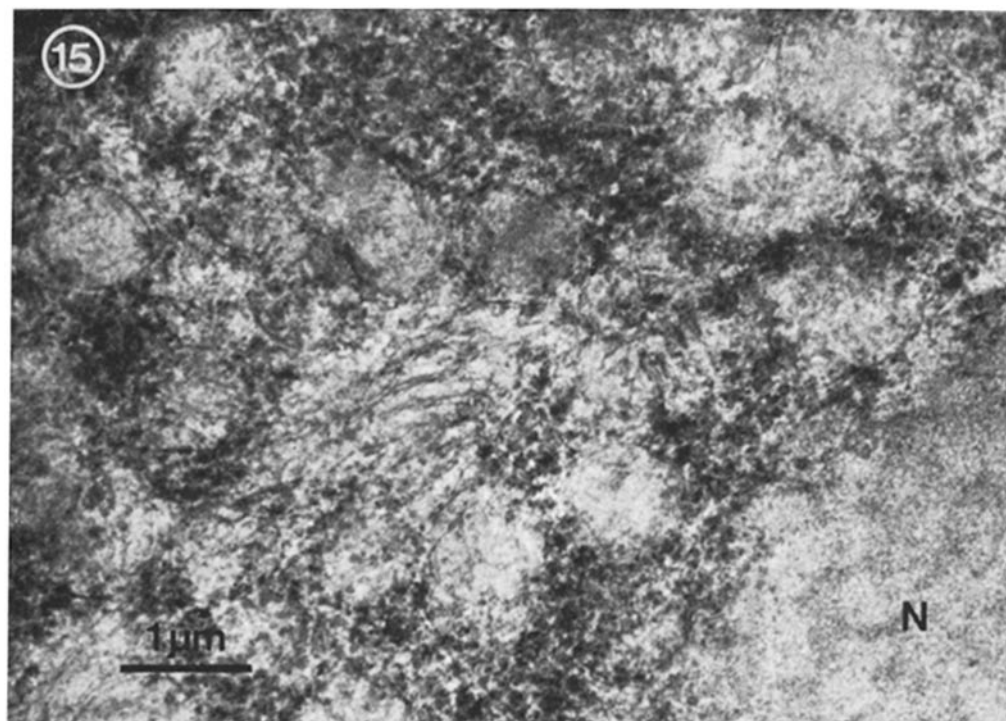

FIGURE 15 Very thick (10 μm) section of rat liver. Stained in the block with uranyl acetate and lead citrate. Little detail is visible as a result of the overlap of structures in depth. N, nucleus. 2 MV. × 17,500. (From Favard et al., 1971, with copyright permission.)
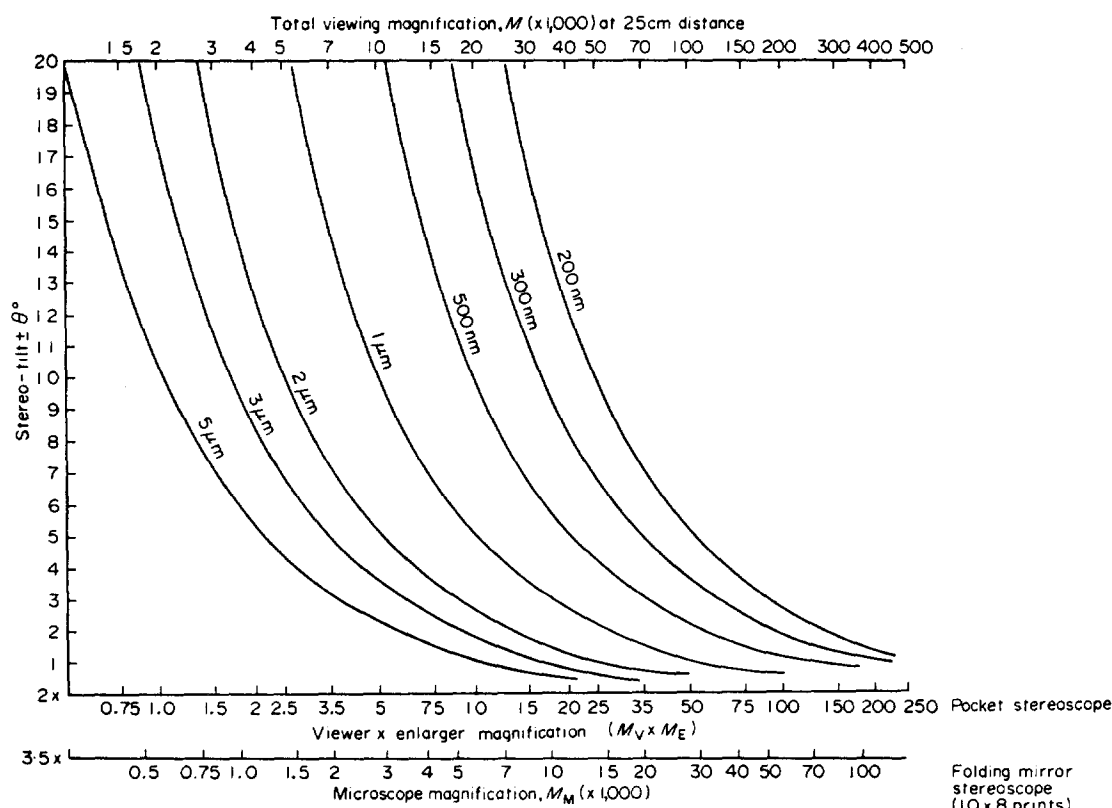
FIGURE 16 Curves giving the optimum stereo tilt angles for a range of *microscope magnifications* and various specimen thicknesses for two common systems of final viewing of stereo pairs. (Abstracted from Hudson and Makin, 1970, by Beeston, 1973, with copyright permission.) To use the chart, first decide the preferred system of final viewing and then read off the optimum tilt angle for the particular specimen thickness and microscope magnification selected, using the appropriate abscissa. (From Beeston, 1973.) Suitable pocket stereoscopes for examining the stereo pairs of micrographs illustrating this review are available from C. F. Casella Co., Regent House, Brittania Walk, London N 1, England, and from suppliers of accessories for electron microscopy.

sectioning. Micrographs of intact yeast cells were published in the very early paper of Van Dorsten et al. (1947), and it is curious that so few studies of intact cells have been made subsequently (Table III). The results obtained have been disappointing. This is due partly to the choice of specimen; most workers have examined intact microorganisms (yeasts, bacteria, fungi, etc.) which are very dense and show little internal structure. In addition, the importance of careful drying has usually been ignored. It is well known from early studies on replicas and from the more recent observations with the scanning electron microscope that serious distortion occurs when organisms are dried in air, even if they have been fixed. As will be seen from Table III, only Ris (1969) and Peachey et al. (1974) in studies of isolated chromosomes (Fig. 19)

and cultured cells (Fig. 20) have published micrographs of specimens which have *not* been air dried. In addition, Ris (1969) and Peachey et al. (1974) have realized the importance of obtaining stereo images in order to be able to study three-dimensional organization and to appreciate the structure of the specimen 'in depth'. The results are very similar to those obtained with thick sections, with the advantage that the specimens have not been exposed to dehydrating agents and embedding media. Individual nucleohistone fibers are clearly visible in intact, isolated chromosomes (Ris, 1969) (Fig. 19), and fine cellular details, such as microfilaments, microtubules, and the unit structure of the plasma membrane, are well preserved and well resolved (Peachey et al., 1974) (Fig. 20).

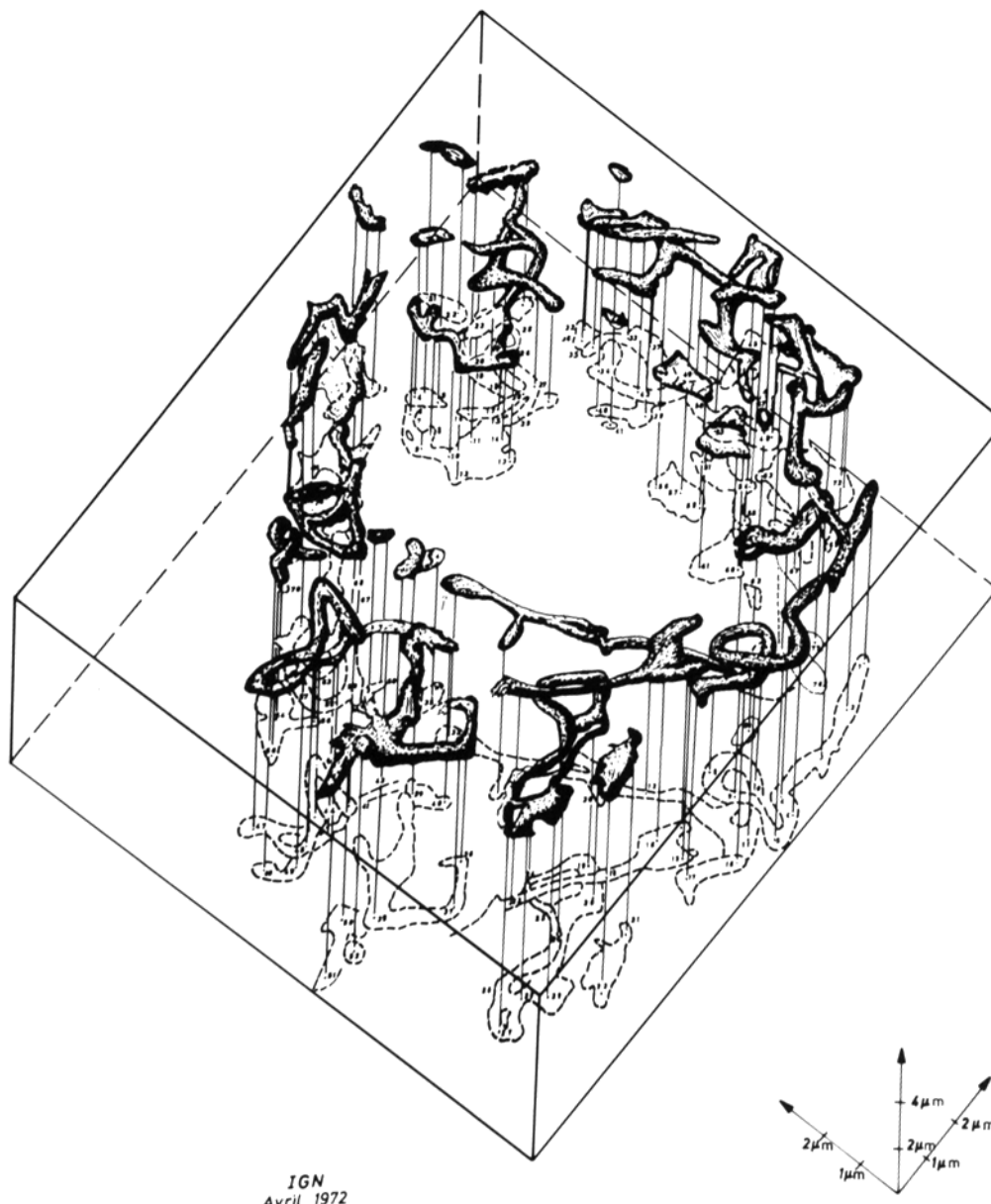Dupouy and his colleagues (Dupouy et al., 1966)

IGN
Avril 1972

FIGURE 17 Stereo model of the forming face of the Golgi apparatus of a small nerve cell, reconstructed from a stereo pair of micrographs of a 7-μm thick section. Stereo tilt angle 10°. (From Rambourg et al., 1973, with copyright permission.)

have shown that greater detail can be observed in intact bacteria and their associated flagella by using the dark-field mode of operation.

Now that the necessity for careful drying has been realized, there is no doubt that this relatively simple preparative technique will be widely used to examine the three-dimensional organization of cells and organelles in the HVEM.

HYDRATED BIOLOGICAL SPECIMENS

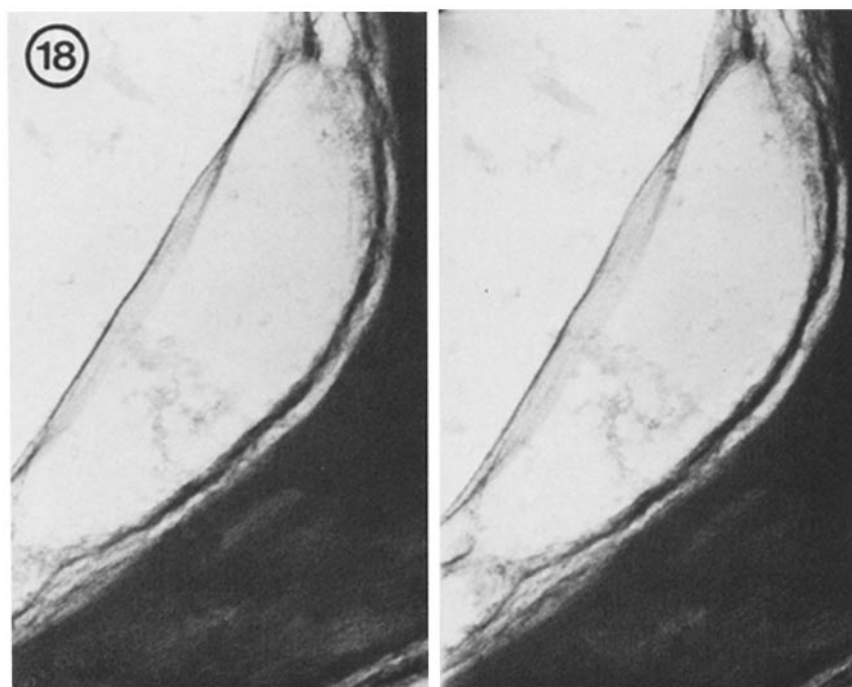The hope that it would be possible to observe living processes was one of the major incentives for the

FIGURE 18 Stereo view of a 1-μm thick section of collenchymatous tissue of a 21-day old celery petiole. The tonoplast has become partially separated from the cytoplasm, allowing an oblique view of the plasma membrane to be obtained. 1 MV. Stereo tilt angle 5°. × 35,000. (From Cox and Juniper, 1973 *a*, with copyright permission.)

TABLE III

Intact Cells and Organelles

Specimen	Fixation and staining	Dehydration	Accelerating voltage	Reference
Yeast cells	–	air-dried	350 kV	Van Dorsten et al. (1947)
Bacteria	–	air-dried	1 MV	Dupouy et al. (1966)
Bacterial spores	–	air-dried	1 MV	Dupouy et al. (1966)
Chromosomes	F; U-Mg-Ac	c-p dried	1 MV	Ris (1969)
Fibroblasts	P + G; U-Mg-Ac	c-p dried	1 MV	Ris, in Cosslett (1971)
Catalase	neg. stain	air-dried	1 MV	Massover (1972 *a*)
Bacterial spores	–	air-dried	800 kV	Hama (1973 *a*)
Mitochondria	neg. stain	air-dried	800 kV	Hama (1973 *a*)
Mushroom hyphae	PTA	air-dried	2.5 MV	Dupouy (1973)
Bacterial spores	–	air-dried	2.5 MV (max)	Nagata and Fukai (1974)
Marine formanifera	?	air-dried	1.2 MV	McGee-Russell and Orville (1974)
Embryonic rat cells	G; OsO₄	c-p dried	1 MV	Peachey et al. (1974)

Key: F, formalin; P, paraformaldehyde; G, glutaraldehyde; U-Mg-Ac, uranyl magnesium acetate; c-p, critical-point; PTA, phosphotungstic acid; neg., negative.

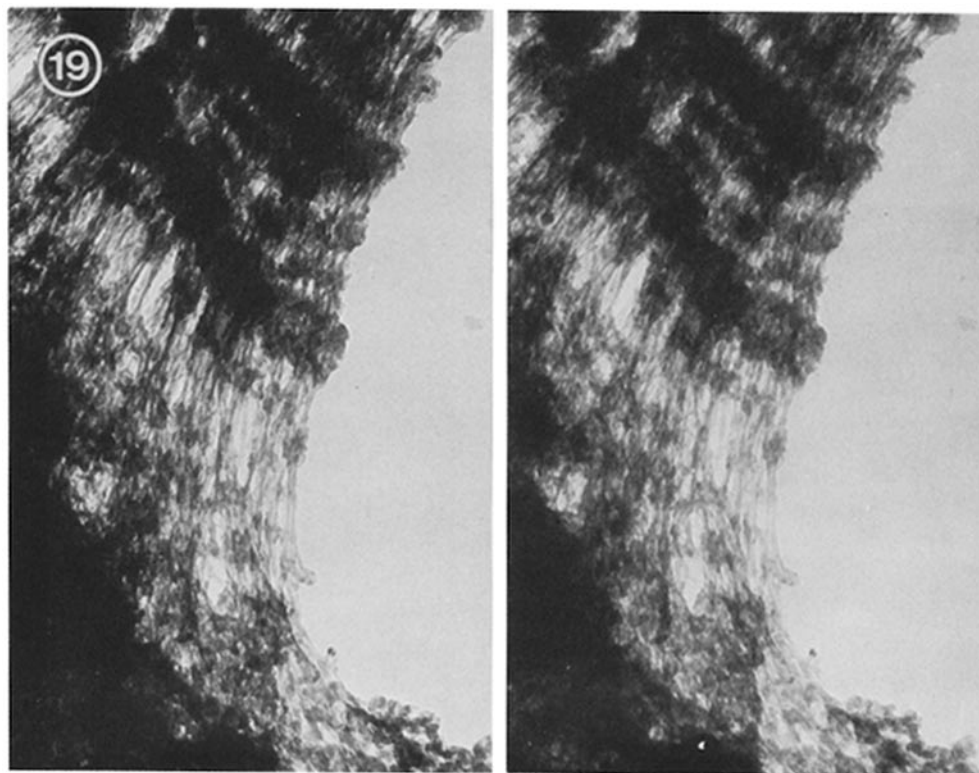Note: the table gives details of published micrographs.

FIGURE 19 Stereo view of part of a salivary gland chromosome of *Drosphila melanogaster;* fixed in formaldehyde, stained with uranyl magnesium acetate and critical-point dried. 1 MV. Stereo tilt angle 10°. × 40,000. (Unpublished micrograph from a study by Hans Ris.)

development of the high voltage electron microscope, and 'living' bacteria were among the first specimens to be examined in the Toulouse 1.5-MV microscope (Dupouy et al., 1960). It is consequently very disappointing that subsequent studies have revealed that there are a number of apparently insuperable problems in any attempt to follow normal cellular processes in the HVEM. There are even considerable difficulties in obtaining single high-resolution images of hydrated specimens, arising from the imaging process itself. These difficulties have become apparent during the examination of biological specimens in suitable environmental cells. These cells are of two types (Fig. 21): the 'aperture' type, in which small apertures are placed above and below the specimen to limit the flow of gas from the specimen area to the microscope column, and the 'window' type, in which electron-transparent windows are placed above and below the specimen so that the specimen and its special environment are sealed off from the

vacuum in the column. Details of the design and operation of environmental cells are reviewed by Flower (1973), Joy (1973), and Parsons (1974 *b*).

The very few accounts of observations of hydrated biological specimens so far published are listed in Table IV. The list includes only papers illustrated with micrographs in which the resolution is comparable with that obtainable by light microscopy. This resolution is limited both by the film of water which covers the specimen when it is in a humid atmosphere and by the damage caused by irradiation with electrons during observation in the microscope.

In order to obtain a sharp image it is necessary to reduce the thickness of the water film, although great care has to be taken not to let the process go too far because drying artifacts will begin to appear (Parsons et al., 1972; Parsons et al., 1974). Tighe et al. (1973) controlled the thickness of the water layer by reducing the pressure within the environmental cell from atmospheric pressure
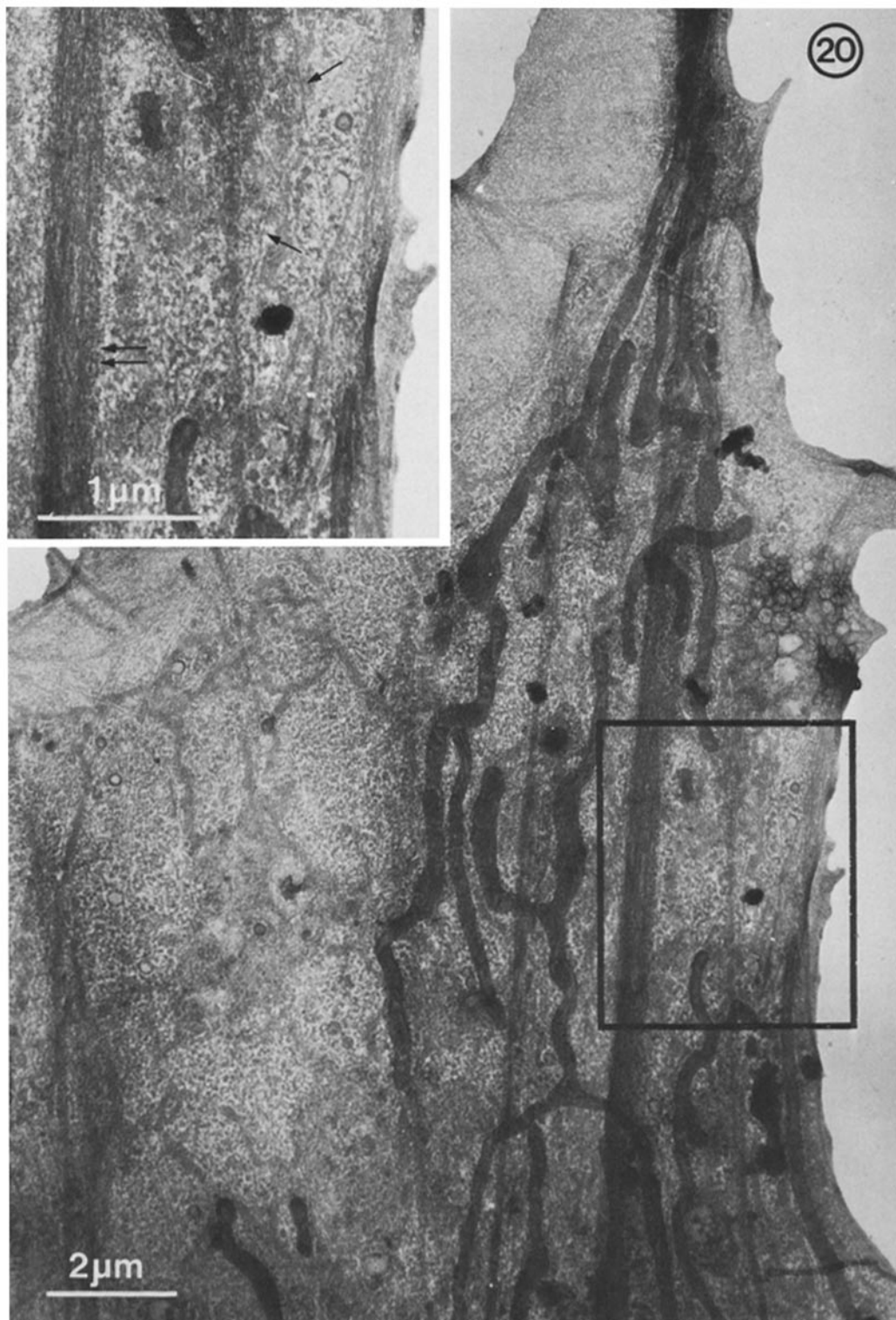
FIGURE 20   An intact rat embryo cell prepared by critical-point drying. Microtubules (arrows) and intra-
cellular filaments (double arrows) are clearly visible. 1 MV. × 10,000. (*Inset*, × 25,000.) (Unpublished
micrograph from a study by Ian Buckley and Keith R. Porter.)

738

down to about 400 torr (Fig. 22). The resolution was still severely limited by the effects of electron bombardment, starch-rich regions of the cells being particularly prone to radiation damage (Fig. 23). This damage was reduced by decreasing the brightness of the image, but the specimens (green algae and red blood cells) could not be examined at magnifications higher than × 10,000. In a study of hydrated fungal spores, Allinson et al. (1973) found that the spores swelled by as much as 25% during the first few seconds of normal viewing at 1 MV and then collapsed. Reduction of the beam intensity from 2×10^{-3} A cm^{-2} to 5×10^{-4} A

cm^{-2} allowed several minutes of observation before any obvious damage was apparent.

Another factor that influences both the resolution and the extent of radiation damage is the thickness of the specimen itself. Since the first observations by Dupouy et al. (1960), there has been a tendency to choose microorganisms (bacteria, algae, etc) or red blood cells (Fig. 24) as test specimens for the HVEM, presumably because they are relatively easy to obtain and because viability tests are readily carried out. The resolution is limited in these cells, however, because they are thick (at least 0.5 μm and often much more) and their cytoplasmic contents are very dense. A far better choice of test specimen was made by Parsons and his colleagues (Parsons et al., 1972; Parsons and Matricardi, 1974; Parsons et al., 1974) who examined mammalian cells (melanoma cells and 3T3 cells) grown on Formvar- and carbon-coated gold grids. Under these conditions the cells spread out thinly and considerable cytoplasmic and nuclear detail is visible (Fig. 25). Methods were tested for reducing the thickness of the water layer on the cells by making regions of the grid hydrophobic. This could sometimes be achieved by washing with saline solutions and was routinely successful after glutaraldehyde fixation (Fig. 26). An obvious danger with this particular
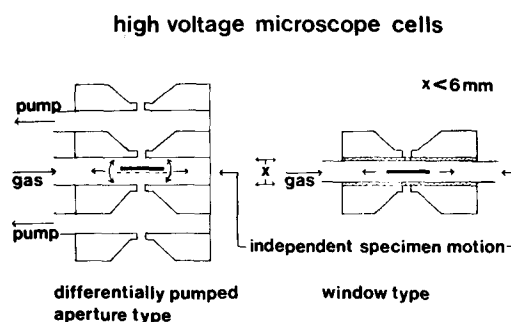
high voltage microscope cells

FIGURE 21 Environmental cells for the high voltage electron microscope. (From Flower, 1973, with copyright permission.)

TABLE IV

Hydrated Specimens

Specimen	Environment	Accelerating voltage	Reference
Bacteria	Saturated water vapour	600–700 kV	Dupouy et al. (1960)
Bacteria	Saturated water vapour	1 MV	Dupouy and Perrier (1962)
Bacteria	Saturated water vapour	1 MV	Dupouy (1968)
Melanoma cells and 3T3 cells	Salt solution; water vapour, plus oxygen and helium; 20–30 torr	800 kV	Parsons et al. (1972)
Bovine sperm	Salt solution; partially dried	800 kV	Parsons et al. (1972)
Catalase	Ammonium molybdate; 'wet' helium	?	Ward and Mitchell (1972)
Fungal spores	'Damp' air or helium; atmospheric pressure	1 MV	Allinson et al. (1973)
Red blood cells	Phosphate buffer; helium; atmospheric pressure	300 kV	Clarke et al. (1973)
Green algae and red blood cells	Water saturated with helium; 400 torr	1 MV	Tighe et al. (1973)
3T3 cells; white blood cells; red blood cells; liver cells	Salt solution; water vapour; 24 torr	800 kV	Parsons et al. (1974); Parsons and Matricardi (1974)

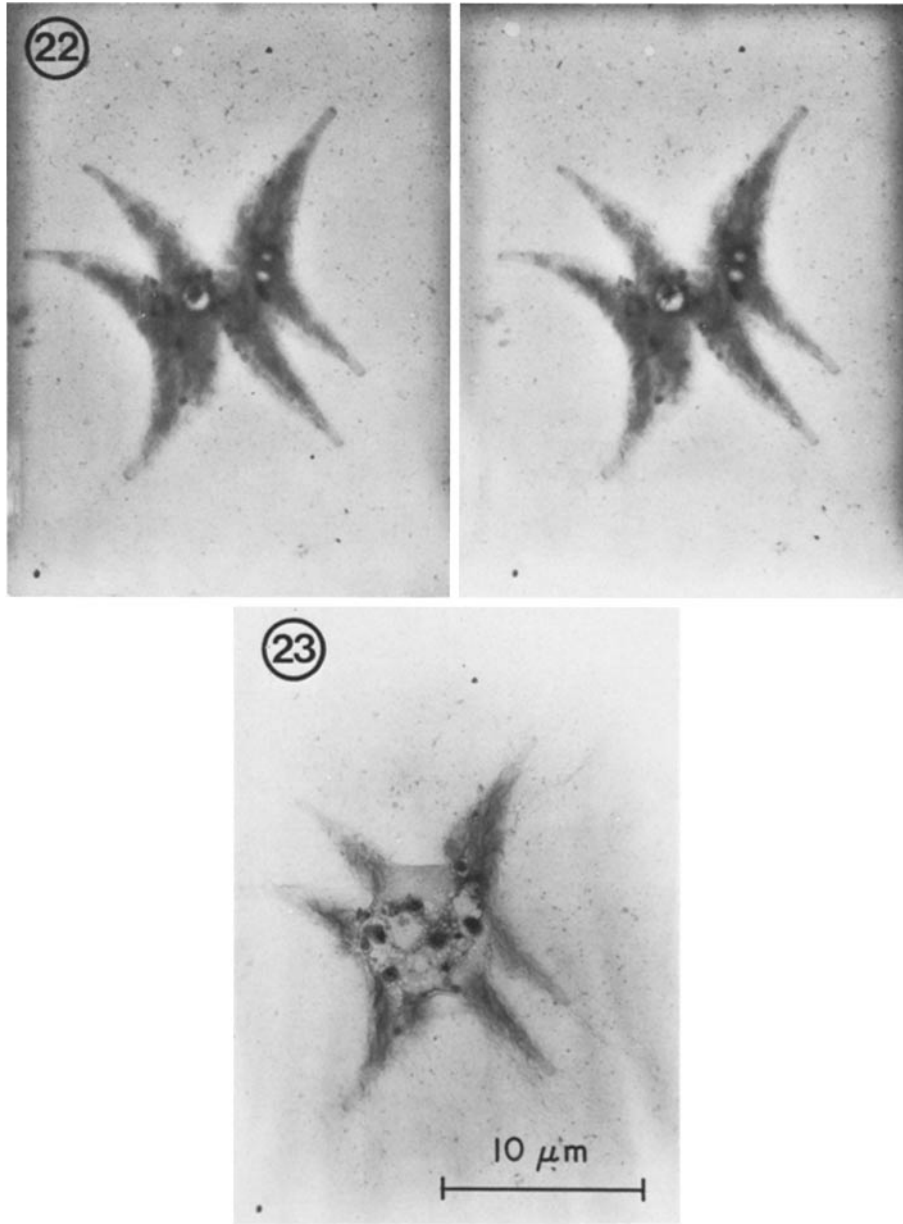Note: the table gives details of published micrographs.

FIGURE 22   Stereo view of a fresh water green alga (*Selenastrum*) in 400 torr of water-saturated helium. Starch-rich regions have been damaged by the electron beam to produce light spherical structures. The small dark bodies may be mitochondria. 1 MV. × 2,700. (From Tighe et al., 1973, with copyright permission.)

FIGURE 23   The same specimen as in Fig. 22. A fully focused beam has produced rapid destruction of the algae within 1 min. 1 MV. × 2,700. (Unpublished micrograph from a study by N. J. Tighe, H. M. Flower, and P. R. Swann.)
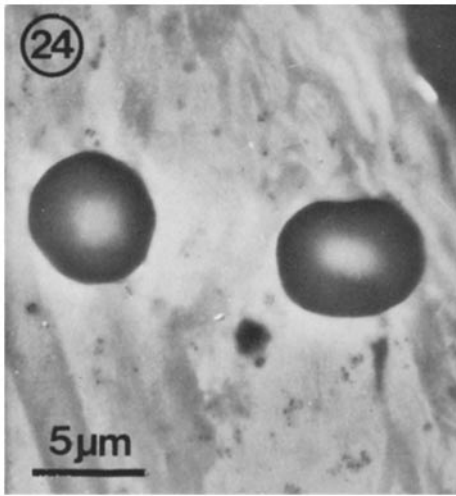
FIGURE 24   Hydrated mouse red blood cells in water vapour at 24 torr pressure have the characteristic disk shape with a thinner central region. 800 kV. × 3,000. (From Parsons et al., 1974, with copyright permission.)
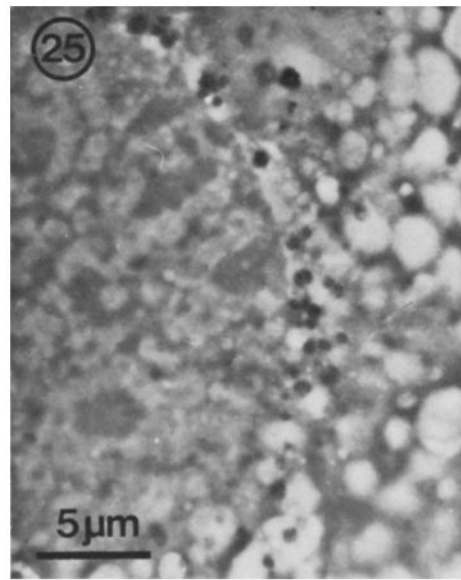

FIGURE 25   Thinly spread liver cell in water vapour at 24 torr pressure. The nucleus is thin enough to show molecular and chromatin structure, but the mitochondria appear swollen. 800 kV. × 3,000. (From Parsons et al., 1974, with copyright permission.)
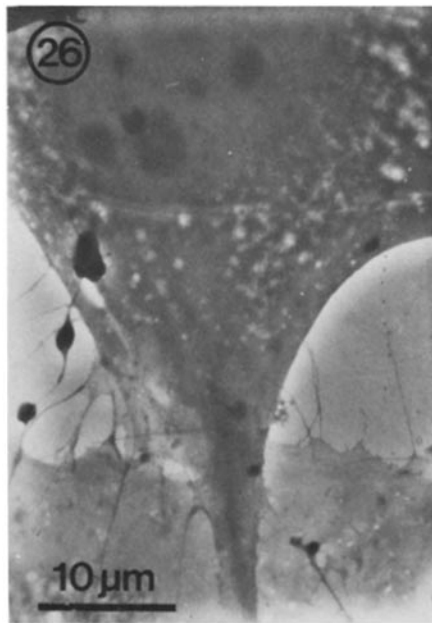

FIGURE 26   Glutaraldehyde-fixed, wet unstained 3T3 cell. Fixation has resulted in the retreat or thinning of the water layer on the surface of the cell, allowing the fine cytoplasmic processes to be clearly seen. Cytoplasmic vesicles and granules appear clumped. 800 kV. × 1,800. (From Parsons et al., 1974, with copyright permission.)
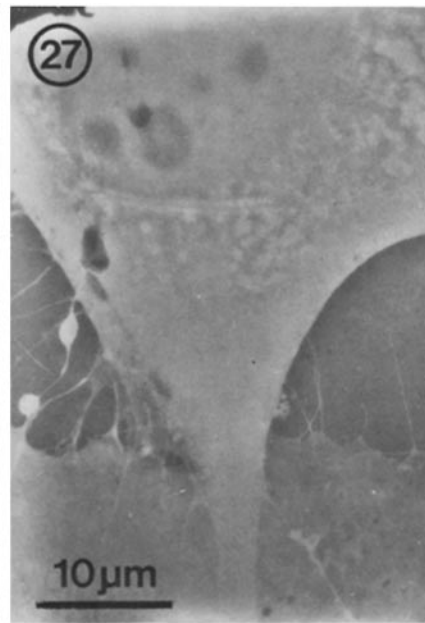
FIGURE 27   Dark-field image of the cell shown in Fig. 26. The retraction of the water layer allows good contrast and resolution of the fine processes to be obtained. 800 kV. 1,800. (From Parsons et al., 1974, with copyright permission.)
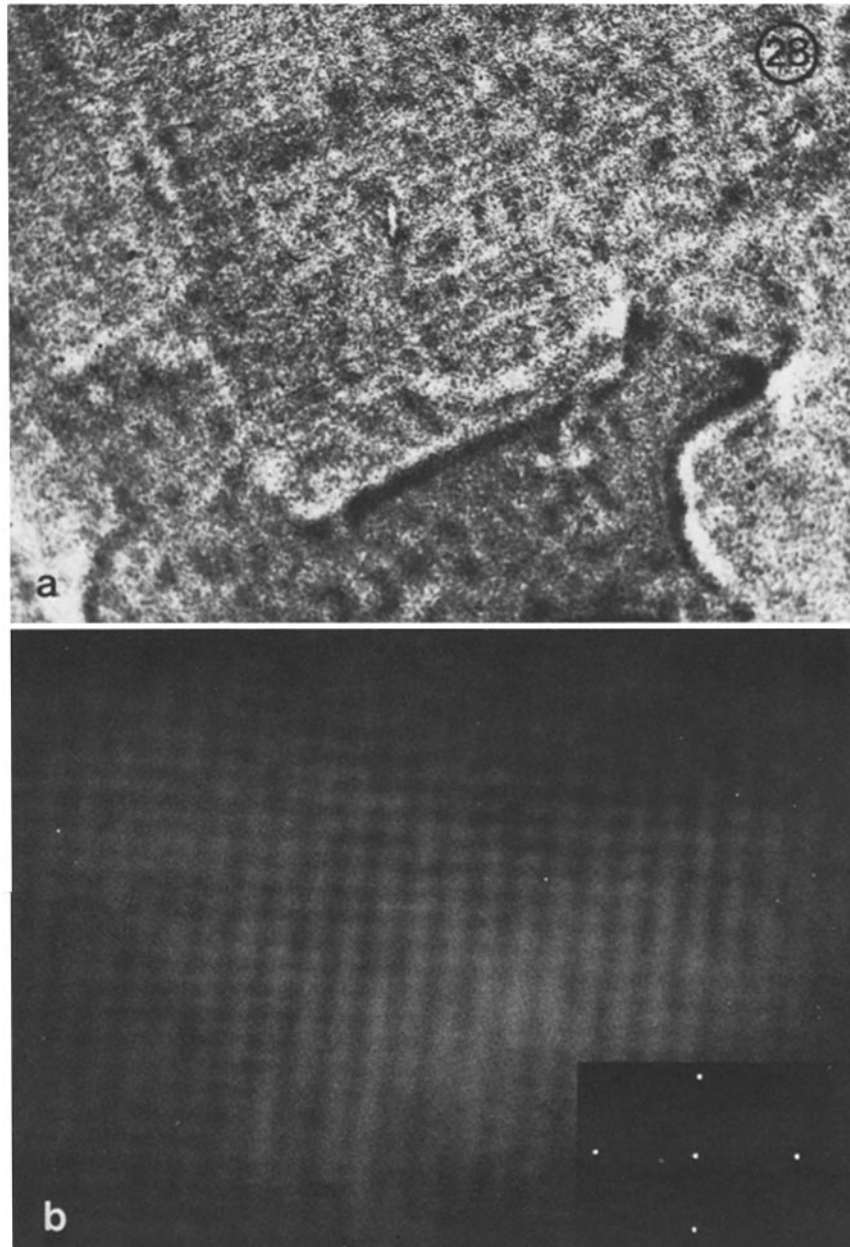
FIGURE 28   (a) A catalase crystal in an atmosphere of 'wet' helium. (b) The averaged image of the catalase crystal in (a). The 8.6-nm × 6.8-nm periods of the crystal are visible. *Inset*: the diffraction filter used in the image processing. (From Ward and Mitchell, 1972, with copyright permission.)

technique is that dehydration may commence after the retraction of the water layer from the cell.

The contrast in these unstained preparations of hydrated cells is very low, but the thinner regions of spread cells can be viewed without loss of resolution in the dark-field mode of operation (Fig. 27). Details of the cell periphery are visible in good contrast.

The highest resolution so far achieved in studies on wet biological specimens in the HVEM was
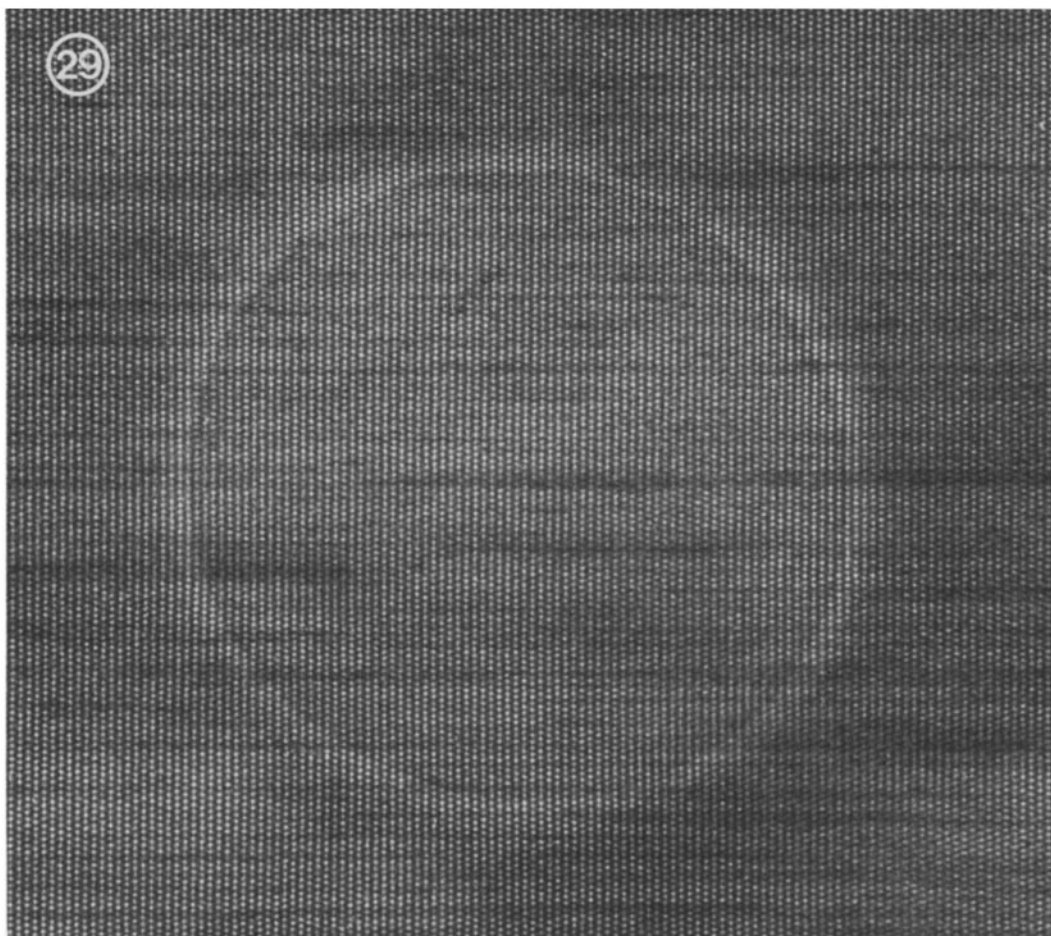
FIGURE 29   Part of a catalase crystal negatively stained with 2% sodium silicotungstate and deposited on a fenestrated carbon film. 1.5 MV (Laboratoire d'Optique, Toulouse). × 125,800. (Unpublished micrograph from a study by William H. Massover.)

obtained by Ward and Mitchell (1972) in an examination of catalase crystals. The catalase was suspended in 1% ammonium molybdate and placed in an environmental cell in an atmosphere of wet helium. Normal beam intensities for viewing caused bubbling and rapid loss of the oblong form of the microcrystals. However, the use of an image intensifier enabled recordings to be made at low-beam intensities, and there was no apparent change in the catalase crystals in the period needed to focus the image. Indications of the 8.6 × 6.8-nm periodicities of the crystals were present in the electron micrographs (Fig. 28 a) and these periodicities were clearly visible after application of optical diffraction and filtering techniques (Fig. 28 b). It is interesting to compare this micrograph

with the images of dry, negatively stained catalase crystals published by Massover (1972 a) (Fig. 29).

The rapidity with which radiation damage becomes apparent in hydrated biological specimens suggests that it will probably not be possible to follow normal dynamic processes in the HVEM. Various cellular movements have been reported, such as the swelling of fungal spores (Allinson et al., 1973), the formation of cellular processes on the surfaces of red cells treated with antibodies (Clarke et al., 1973), and the division of bacteria (Clarke et al., 1973), and some of these movements have been recorded on videotape (Salsbury et al., 1974).

The thinly spread cells studied by Parsons and his colleagues (Parsons et al., 1972; Parsons and

Table V

Imaging Requirements and Radiation Damage at 1 MV

Resolvable structures, assuming 10% contrast	Minimal electron exposure required for detectability (coulomb/cm²)	Rad dose/picture corresponding to electron exposure on the left (stopping power calculation)	Biological effect
	10⁻¹⁰		
Whole cells (10 μm) →			
	10⁻⁹	100	
			← Reproductive cell death (animal cells)
Cell nucleus (2 μm) →	10⁻⁸	10³	
			← Inactivation of T1 bacteriophage
	10⁻⁷	10⁴	
Mitochondrion (5,000 Å) →			← Reproductive cell death (E. coli)
	10⁻⁶	10⁵	⎬ Enzyme inactivation
Tumor virus (1,000 Å) →			
	10⁻⁵	10⁶	← Stoppage of cell motility (protozoa)
			← Reproductive death (Micrococcus radiodurans)
Ribosomes, chromatin fibers (200 Å) →	10⁻⁴	10⁷	
Cell membranes (100 Å) →		10⁸	
Enzymes (50 Å) →	10⁻³		
Nucleic acids (25 Å) →	10²	10⁹	
10-Å resolution →		10¹⁰	
5-Å resolution →	10¹		
	1	10¹¹	

(From Glaeser, 1974.)

Matricardi, 1974; Parsons et al., 1974) appeared completely static. This was attributed to the unphysiological conditions within the environmental cell, but may also have been due to surface tension forces exerted by the thin water film (Joy, 1973).

It seems most unlikely that the cellular movements observed in the HVEM are significant in terms of living processes (Glaeser, 1974). Bacteria which have received a lethal dose of radiation will often go through one or more subsequent division processes, but these are usually bizarre and do not indicate 'viability' in the accepted sense of the word. Experiments in which organisms have been irradiated by viewing in the electron microscope

and then removed and incubated in culture medium (Dupouy et al., 1960; Nagata and Ishikawa, 1971; Nagata and Fukai, 1974) must also be examined carefully. Unless steps are taken to view the same organisms after irradiation, misleading results may be obtained since not all the organisms in the environmental cell may have been irradiated. Also, any subsequent 'growth' (or germination of spores) is just as likely to be abnormal as for organisms observed continuously in the microscope.

The information that is available from the extensive literature on the effects of radiation on living cells indicates that there is very little promise of observing normal living processes in the electron microscope at a resolution higher than that attainable in the light microscope. The dose received by the specimen during observation and recording in the electron microscope is excessive in biological terms. For example, Grubb and Keller (1972) have estimated that the irradiation received by the specimen during the recording of a single micrograph is equivalent to 5 wk of irradiation within a nuclear pile, or to 5 yr near a 1-Ci $Co^{60}\gamma$-ray source, or to the irradiation from a 10-megaton H bomb exploded about 30 yards away! The situation has also been clearly illustrated by Glaeser (1974) in a table (Table V) in which the minimum electron exposure required to obtain a single micrograph at a particular resolution is compared with the known biological effects of the corresponding dose of radiation. The electron exposure increases as the resolution increases and becomes lethal to all known organisms long before it is possible to visualize cell membranes. Glaeser (1974) concludes that only structures larger than 1 μm can be observed with relatively little radiation damage and that it is doubtful whether structures smaller than 100 nm can be seen in a state that can be referred to as 'living'.

CONCLUSIONS

It is hoped that this review has clearly demonstrated the considerable potentiality of the high voltage electron microscope to make significant contributions in biology. To date, the major achievement has been the three-dimensional image of biological structures provided by stereo viewing of thick specimens. A few minutes' examination of the stereo pairs of micrographs that illustrate this review will indicate the value of the technique, which has already been applied to over 35 very

different specimens (Table II). There seems no doubt that, once they have become familiar with the three-dimensional appearance of their specimens, biologists will no longer be satisfied with the information provided by thin sections alone. In consequence, the HVEM examination of thick sections promises to become soon one of the standard techniques of biological electron microscopy.

The other applications of the HVEM in biology are at earlier stages of development, but the relatively little work so far done has already indicated that the HVEM will make significant contributions both in studies of thin specimens at high resolution and in the examination of biological material in the hydrated state.

REFERENCES

ALLINSON, D. L., M. S. LOVEDAY, and A. W. O. GOSNOLD. 1973. Applications of the NPL Environmental cell for use in the AEI EM7 1 MeV electron microscope. *J. Microsc. (Oxf.).* **97:**209-216.

BEESTON, B. E. P. 1973. High voltage microscopy of biological specimens: some practical considerations. *J. Microsc. (Oxf).* **98:**402-416.

CARASSO, N., M.-C. DELAUNAY, P. FAVARD, and J.-P. LECHAIRE. 1973. Obtention et coloration de coupes épaisses pour la microscopie électronique a haute tension. *J. Microsc. (Paris).* **16:**257-268.

CARASSO, N., P. FAVARD, P. MENTRÉ, and N. POUX. 1974. High voltage transmission electron microscopy of cell compartments in Araldite thick sections. Pro-

ceedings of the 3rd International Congress on High Voltage Electron Microscopy, Oxford. 414–418.

CARASSO, N., L. OVTRACHT, and P. FAVARD. 1971. Observation, en microscopie électronique haute tension, de l'appareil de Golgi sur coupes de 0.5 à 5µ d'épaisseur, C. R. Hebd. Seances Acad. Sci. 273D: 876–879.

CLARKE, J. A., P. R. WARD, and A. J. SALSBURY. 1973. High voltage electron microscopy of cellular changes in the wet state. J. Microsc. (Oxf.). 97:365–368.

COSSLETT, V. E. 1969. High-voltage electron microscopy. Q. Rev. Biophys. 2:95–133.

COSSLETT, V. E. 1971. High voltage electron microscopy and its application in biology. Philos. Trans. R. Soc. Lond. Ser. B Biol. Sci. 261:35–44.

COSSLETT, V. E. 1974 a. Perspectives in high voltage electron microscopy. Proc. R. Soc. Lond. A. 338:1–16.

COSSLETT, V. E. 1974 b. Current developments in high voltage electron microscopy. J. Microsc. (Oxf.). 100:233–246.

COX, G., and B. JUNIPER. 1973 a. The application of stereo-micrography in the high voltage electron microscope to studies of cell-wall structure and deposition. J. Microsc. (Oxf.). 97:29–40.

COX, G., and B. JUNIPER. 1973 b. Electron microscopy of cellulose in entire tissue. J. Microsc. (Oxf.) 97:343–355.

DRUMMOND, D. G., editor. 1950. The practice of electron microscopy. J. R. Microsc. Soc. 70:1–141.

DUPOUY, G. 1968. Electron microscopy at very high voltages. Adv. Opt. Electron Microsc. 2:167–250.

DUPOUY, G. 1973. Performance and applications of the Toulouse 3 million volt electron microscope. J. Microsc. (Oxf.), 97:3–28.

DUPOUY, G. 1974. Megavolt electron microscopy. Proceedings of the 3rd International Congress on High Voltage Electron Microscopy, Oxford. 441–457.

DUPOUY, G., and F. PERRIER. 1962. Microscope électronique fonctionnant sous une tension d'un million de volts. J. Microsc. (Paris). 1:167–192.

DUPOUY, G., F. PERRIER, and L. DURRIEU. 1960. Microscopie électronique. L'observation de la matière vivante au moyen d'un microscope électronique fonctionnant sous très haute tension. C. R. Hebd. Seances Acad. Sci. 251:2836–2841.

DUPOUY, G. F. PERRIER, L. ENJALBERT, L. LAPCHINE, and P. VERDIER. 1969. Accroisement du contraste des images d'objets amorphes en microscopie électronique. C. R. Hebd. Seances Acad. Sci. 268B:1341–1345.

DUPOUY, G., F. PERRIER, and P. VERDIER. 1966. Amélioration du contraste des images d'objets amorphes minces en microscopie électronique. J. Microsc. (Paris). 5:655–668.

FAVARD, P. and N. CARASSO. 1973. The preparation and observation of thick biological sections in the high voltage electron microscope. J. Microsc. (Oxf.). 97:59–81.

FAVARD, P., L. OVTRACHT, and N. CARASSO. 1971. Observations de spécimens biologiques en microscopie électronique a haute tension. 1. Coupes épaisses. J. Microsc. (Paris). 12:301–316.

FLOWER, H. M. 1973. High voltage electron microscopy of environmental reactions. J. Microsc. (Oxf.). 97:171–190.

FRIEND, D. S., and M. J. MURRAY, 1965. Osmium impregnation of the Golgi apparatus. Am. J. Anat. 117:135–150.

GLAESER, R. M. 1974. Radiation damage and biological electron microscopy. In Electron Microscopy 1973. B. Siegel, editor. John Wiley and Sons, Inc., New York. In press.

GLAUERT, A. M. 1971. The electron microscope in biology, 1971. Proceedings of the 25th Anniversary Meeting EMAG/IOP. 188–193.

GLAUERT, A. M. 1972. High power microscopy and the role of the Royal Microscopical Society. Proc. R. Microsc. Soc. 7:193–206.

GLAUERT, A. M., and C. R. MAYO. 1973 . The study of the three-dimensional structural relationships in connective tissues by high voltage electron microscopy. J. Microsc. (Oxf.). 97:83–94.

GRUBB, D. T., and A. KELLER. 1972. Beam-induced radiation damage in polymers and its effect on the image formed in the electron microscope. Proceedings of the 5th European Regional Conferences on Electron Microscopy, Manchester. 554–560.

HAMA, K. 1973 a. High voltage electron microscopy. In Advanced Techniques in Biological Electron Microscopy. J. K. Koehler, editor. Springer-Verlag, Berlin. 275–297.

HAMA, K. 1973 b. A study of the fine structure of the lateral line organ of the sea eel. Proceedings of the 31st Annual Meeting of the Electron Microscopy Society of America. 648–649.

HAMA, K., and T. KAMINO. 1974. Three-dimensional observation of sensory hairs of the lateral line canal organ of the sea eel using thick serial sections. Proceedings of the 3rd International Congress on High Voltage Electron Microscopy, Oxford. 423–425.

HAMA, K., and F. NAGATA. 1970 a. High resolution observation of biological sections with a high voltage electron microscope. J. Electron Microsc. 19:170–175.

HAMA, K., and F. NAGATA, 1970 b. A stereoscope observation of tracheal epithelium of mouse by means of the high voltage electron microscope. J. Cell Biol. 45:654–659.

HAMA, K., and F. NAGATA. 1970 c. Stereoscope observations of the biological specimens by means of high voltage electron microscope, Proceedings of the 7th International Congress on Electron Microscopy, Grenoble. 1:461–462.

HAMA, K., and K. R. PORTER. 1969. An application of high voltage electron microscopy to the study of biological materials. J. Microsc. (Paris). 8:149–158.

HUDSON, B., and M. J. MAKIN. 1970. The optimum tilt angle for electron stereo-microscopy. *J. Phys. E. Sci. Instrum.* **3**:311.

JOY, R. T. 1973. The electron microscopical observation of aqueous biological specimens. *Adv. Opt. Electron Microsc.* **5**:297–352.

KING, R. C., and H. AKAI. 1971. Observations of meiotic chromosomes with an ultra-high voltage electron microscope. *JEOL News.* **9**:12–15.

LOCKE, M., and N. KRISHNAN. 1971. Hot alcoholic phosphotungstic acid and uranyl acetate as routine stains for thick and thin sections. *J. Cell Biol.* **50**:550–557.

LOCKE, M., N. KRISHNAN, and J. T. MCMAHON. 1971. A routine method for obtaining high contrast without staining sections. *J. Cell Biol.* **50**:540–544.

MASSOVER, W. H. 1972 *a*. Ultra-high voltage electron microscopy (1–3 MeV) of biological macromolecules. Proceedings of the 30th Annual Meeting of the Electron Microscopy Society of America. 182–183.

MASSOVER, W. H. 1972 *b*. On the high voltage electron microscopy (1 MeV) of biological thick sections. Stereoscopic examination. Proceedings of the 30th Annual Meeting of the Electron Microscopy Society of America. 464–465.

MASSOVER, W. H. 1973. Complex surface invaginations in frog oocytes. *J. Cell Biol.* **58**:485–491.

MASSOVER, W. H. 1974. Effective resolution in biological thin sections: experimental results with ultra-high voltage electron microscopy (1–3 MeV). Proceedings of the 3rd International Congress on High Voltage Electron Microscopy, Oxford. 163–166.

MASSOVER, W. H., J.-C. LACAZE, and L. DURRIEU. 1973. The ultrastructure of ferritin macromolecules. I. Ultrahigh voltage electron microscopy (1–3 MeV). *J. Ultrastruct. Res.* **43**:460–475.

MAYO, C. R., and B. E. P. BEESTON. 1971. Some aspects of the biological application of high voltage electron microscopy. Proceedings of the 29th Annual Meeting of the Electron Microscopy of Society of America. 470–471.

MCGEE-RUSSELL, S. M., and R. E. ORVILLE. 1974. Aspects of image analysis of high voltage electron micrographs of air-dried whole mounts of pseudopodial networks of the marine protozoan *Allogromia* (*Formanifera*). Proceedings of the 3rd International Congress on High Voltage Electron Microscopy, Oxford. 155–162.

NAGATA, F., and K. FUKAI. 1974. Irradiation effects and penetration of non-metallic materials at high voltages. Proceedings of the 3rd International Congress on High Voltage Electron Microscopy, Oxford. 379–382.

NAGATA, F., and K. HAMA. 1969. Observation of biological specimens with a high voltage electron microscope. Proceedings of the 27th Annual Meeting of the Electron Microscopy Society of America. 98–99.

NAGATA, F., K. HAMA, and K. R. PORTER. 1969. Three

dimensional observation of biological specimen with high voltage electron microscopy. *J. Electron Microsc.* **18**:106–109.

NAGATA, F., and F. ISHIKAWA. 1971. High voltage electron microscope study of living materials. Proceedings of the 29th Annual Meeting of the Electron Microscopy Society of America. 464–465.

PALAY, S. L., and V. CHAN-PALAY. 1973. High voltage electron microscopy of the central nervous system in Golgi preparations. *J. Microsc. (Oxf.).* **97**:41–47.

PARSONS, D. F. 1974 *a*. Radiation damage in biological material. *In* Electron Microscopy, 1973. Physical Aspects. B. Siegel, editor. John Wiley and Sons, Inc., New York. In press.

PARSONS, D. F. 1974 *b*. Environmental wet cells for biological medium voltage and high voltage electron microscopy. *In* Electron Microscopy, 1973. Physical Aspects. B. Siegel, editor. John Wiley and Sons, Inc., New York. In press.

PARSON, D. F., and V. R. MATRICARDI. 1974. Environmental wet cells. Proceedings of the 3rd International Congress on High Voltage Electron Microscopy, Oxford. 396–402.

PARSONS, D. F., V. R. MATRICARDI, J. SUBJECK, I. UYDESS, and G. WRAY. 1972. High-voltage electron microscopy of wet whole cancer and normal cells. *Biochim. Biophys. Acta.* **290**:110–124.

PARSONS, D. F., I. UYDESS, and V. R. MATRICARDI. 1974. High voltage electron microscopy of wet whole cells. Effect of different wet cell preparation methods on visibility of structures. *J. Microsc. (Oxf.).* **100**:153–167.

PEACHEY, L. D., M. FOTINO, and K. R. PORTER. 1974. Biological applications of high voltage electron microscopy. Proceedings of the 3rd International Congress on High Voltage Electron Microscopy, Oxford. 405–413.

RAMBOURG, A., and M. CHRÉTIEN. 1970. L'appareil de Golgi; examen en microscopie électronique de coupes épaisses (0.5–1μ) après impregnation de tissus par le tétroxyde d'osmium. *C. R. Acad. Sci.* **270D**:981–983.

RAMBOURG, A., A. MARRAUD, and M. CHRÉTIEN. 1973. Tri-dimensional structure of the forming face of the Golgi apparatus as seen in the high voltage electron microscope after osmium impregnation of the small nerve cells in the semilunar ganglion of the trigeminal nerve. *J. Microsc. (Oxf.).* **97**:49–57.

RAMBOURG, A., A. MARRAUD, and Y. CLERMONT. 1974. Three-dimensional aspects of the forming face of the Golgi apparatus as seen in the high voltage electron microscope after osmium impregnation. Proceedings of the 3rd International Congress on High Voltage Electron Microscopy, Oxford. 419–422.

REID, N. 1974. Ultramicrotomy. *In* Practical Methods in Electron Microscopy. A. M. Glauert, editor. North-Holland, Amsterdam.

RIS, H. 1969. Use of the high voltage electron micro-

scope for the study of thick biological specimens. *J. Microsc. (Paris)*. **8**:761-766.

SALSBURY, A. J., P. R. WARD, and J. A. CLARKE. 1974. Observations of human red blood cells and bacteria in a controlled environment. Proceedings of the 3rd International Congress on High Voltage Electron Microscopy, Oxford. 403-404.

SZIRMAE, A., R. M. FISHER, J. MOSES, and R. V. RICE. 1971. Contrast and resolution of thick sections of muscle in the HVEM. Proceedings of the 29th Annual Meeting of the Electron Microscope Society of America. 462-463.

THOMAS, L. E., S. LENTZ, and R. M. FISHER. 1974. Stereoscopic methods in the HVEM. Proceedings of the 3rd International Congress on High Voltage Electron Microscopy, Oxford. 255-259.

TIGHE, N. J., H. M. FLOWER, and P. R. SWANN. 1973. An environmental wet cell for high voltage electron microscopy. Proceedings of the 31st Annual Meeting of the Electron Microscopy Society of America. 18-19.

VAN DORSTEN, A. C., W. J. OOSTERKAMP, and J. B. LE POOLE. 1947. An experimental electron microscope for 400 kilovolts. *Philips Technical Rev.* **9**:193-201.

VENABLE, J. H., and R. COGGESHALL. 1965. A simplified lead citrate strain for use in electron microscopy. *J. Cell Biol.* **25**:407-408.

WARD, P. R., and R. F. MITCHELL. 1972. A facility for electron microscopy of specimens in controlled environments. *J. Phys. E. Sci. Instrum.* **5**:160-162.

YAMADA, E., and H. ISHIKAWA. 1972. High voltage electron microscopy for thick sections of biological material combined with molecular tracers. Proceedings of the 30th Annual Meeting of the Electron Microscopy Society of America. 480-481.